United States Department of Agriculture

Statistical Models for the Distribution of Modulus of Elasticity and Modulus of Rupture in Lumber with Implications for Reliability Calculations

Steve P. Verrill
Frank C. Owens
David E. Kretschmann
Rubin Shmulsky

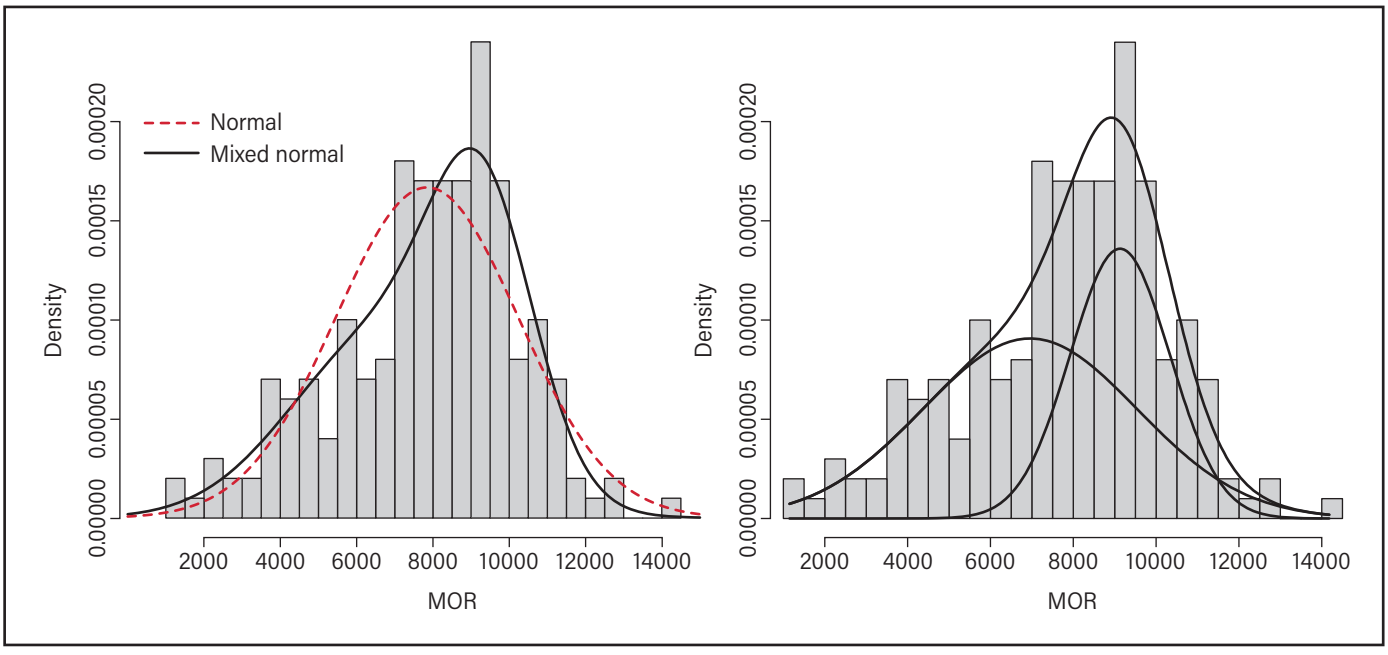

Forest Service
Forest Products Laboratory
Research Paper FPL–RP–692
December 2017

Abstract

It is common practice to assume that a two-parameter Weibull probability distribution is suitable for modeling lumber properties. Verrill and co-workers demonstrated theoretically and empirically that the modulus of rupture (MOR) distribution of visually graded or machine stress rated (MSR) lumber is not distributed as a Weibull. Instead, the tails of the MOR distribution are thinned via "pseudo-truncation." The theoretical portion of Verrill's argument was based on the assumption of a bivariate normal–Weibull (Gaussian–Weibull) MOE–MOR distribution for the full population of lumber (as opposed to the bivariate distribution of visual or MSR grades of lumber). We felt that it was important to investigate this assumption. In the absence of data sets in the literature that were drawn from the full population at a mill, we determined to obtain such a sample for analysis. In this paper, we report the results from this analysis. From the current experiment on mill run lumber, we conclude that if reliability engineers are entertaining the idea of obtaining new efficiencies via careful probability modeling of strength properties, then additional experimental research must be done on the fundamental question of valid models for stiffness and strength distributions for full populations of lumber from a single mill on a single day. Further, we suspect that even if research determines that a simple model can characterize such a distribution, further research will determine that this simple model varies from day to day, mill to mill, and region to region so that an ever-changing mixture model is the correct model. In this case, to ensure that reliability goals are efficiently met, reliability engineers might need to develop detailed computer models that yield real-time, in-line estimates of lumber strength based on measurements of stiffness, specific gravity, knot size and location, slope of grain, and other strength predictors.

Keywords: normal distribution, mixed normal distribution, two-parameter Weibull distribution, three-parameter beta distribution, skew normal distribution, mixed bivariate normal distribution, bivariate Gaussian–Weibull distribution, pseudo-truncated Weibull distribution, machine stress rated data, MSR data, probability density functions, goodness-of-fit, mill run, thin tail, lumber property distribution

Contents

December 2017

Verrill, Steve P.; Owens, Frank C.; Kretschmann, David E.; Shmulsky, Rubin. 2017. Statistical models for the distribution of modulus of elasticity and modulus of rupture in lumber with implications for reliability calculations. Research Paper FPL-RP-692. Madison, WI: U.S. Department of Agriculture, Forest Service, Forest Products Laboratory. 51 p.

A limited number of free copies of this publication are available to the public from the Forest Products Laboratory, One Gifford Pinchot Drive, Madison, WI 53726-2398. This publication is also available online at www.fpl.fs.fed.us. Laboratory publications are sent to hundreds of libraries in the United States and elsewhere.

The Forest Products Laboratory is maintained in cooperation with the University of Wisconsin.

Statistical Models for the Distribution of Modulus of Elasticity and Modulus of Rupture in Lumber with Implications for Reliability Calculations

Steve P. Verrill, Mathematical Statistician
USDA Forest Service, Forest Products Laboratory, Madison, WI

Frank C. Owens, Assistant Research Professor
Department of Sustainable Bioproducts, Mississippi State University

David E. Kretschmann, Research General Engineer (retired[1])
USDA Forest Service, Forest Products Laboratory, Madison, WI

Rubin Shmulsky, Professor and Department Head
Department of Sustainable Bioproducts, Mississippi State University

1 Introduction

Wood reliability engineers have commonly modeled modulus of elasticity (MOE) as a normal distribution and modulus of rupture (MOR) as a normal, lognormal, or two-parameter Weibull distribution (Green and Evans 1987; Evans *et al.* 1997; ASTM 2010, 2015a). However, Verrill *et al.* (2014, 2015) established that even if the strength distribution of the *full* MOR population were a two-parameter Weibull, the strength distributions of subpopulations formed by visual grading or machine stress rating (MSR) would *not* be two-parameter Weibulls. Instead, they would be relatively "thin-tailed" pseudo-truncated Weibulls. Verrill *et al.* (2014) further established that if one fits a two-parameter Weibull to pseudo-truncated Weibull data, estimates of probabilities of breakage when loads are at "allowable" limits (see, for example, ASTM (2016)) can be seriously in error.

We note that the Verrill *et al.* work depends on the assumption that the full bivariate MOE-MOR population has a bivariate Gaussian–Weibull (normal–Weibull) distribution. We felt that it was quite important to investigate this assumption. However, we could find no reports in the literature of studies in which the full MOE-MOR joint distribution or the full marginal distributions were sampled. Instead, samples have been obtained for specific visual grades or specific MSR limits.

Consequently, we determined that it was important to obtain a sample from a full "mill run" bivariate MOE-MOR population. For our initial study, we decided to restrict ourselves to the population of lumber produced at a single mill during a single day. We realize that populations obtained over multiple days from multiple mills in multiple regions are almost certain to have a more complicated structure. However, we felt that it would be useful to first address the fundamental question of whether a "simple" population could be modeled by a "simple" distribution such as a normal or two-parameter Weibull. Thus, in this paper, we report the MOE-MOR data and the distribution fits for a sample of 200 pieces of "mill run" 2x4 lumber obtained from a single mill on a single day.

[1] now President, American Lumber Standard Committee, Inc., Frederick, MD

2 Materials and Methods

Two hundred kiln dried, rough-sawn southern yellow pine (*Pinus* spp.) 2x4s were procured from a large regional sawmill in central Mississippi.

The dimension mill that donated the lumber has a single line primary breakdown followed by a curve gang resaw. It produces 2x4 through 2x12 pine dimension lumber from its log supply. Its annual production is approximately 200 million board feet. The mill is optimized to a large degree throughout with the intention of maximizing board foot recovery from each log.

Mill managers were unaware of the objectives of the research. The mill was asked to pull 200 pieces of 2x4 lumber as the material was removed from the kiln and taken off sticks. The material was removed from the production line after kiln drying but prior to the planing and grading stations. All material was of sufficient character to make it through the optimizing edger and trimmer. Subject only to this condition, the quality of the pieces was unrestricted (the pieces were drawn from the full lumber population rather than from a single grade) and the resulting specimens constitute a full "mill run" sample.

Although the material was not pulled in accord with a random sampling scheme, we believe that the mechanical shuffling of lumber prior to the unscrambler and the kiln stacker randomized the pieces. It can be argued that the material represents a random sample from several hours of a day's production.

The rough dry target dimensions for the mill were 1.7 x 3.7 in. (4.32 x 9.40 cm). The nominal length of the specimens was 8 ft (244 cm), with approximately 1 in. (2.54 cm) of overlength.

The material was transported to Mississippi State University where it was planed on all four sides to final dressed dimensions of 1.5 x 3.5 in. (3.81 x 8.89 cm). Although the material was selected from production and tested as mill-run lumber, the material was graded after planing by a Southern Pine Inspection Bureau (SPIB) certified inspector to provide additional data for future analyses. A visual grade was recorded for each piece. Each board was labeled with a unique identification number and pre-marked to indicate the positioning of the specimen within the third-point bending fixture used in destructive testing. First, the positioning of the 59.5-in. (151.13-cm) test span within the 8-ft-long specimen was determined by a randomly generated number and marked on the top edge of each test piece. This action ensured random placement of the maximum bending moment along the length of each board. Then the corresponding load head positions were marked. Finally, the lumber was stacked unwrapped outside on wooden saw horses under a covered breezeway to protect it from the elements, aid in moisture equalization, and minimize further drying associated with interior storage.

Universal testing machine fixturing and destructive testing procedures were performed in accordance with ASTM D198-15 per the Flexure Test Method (ASTM 2015b). Nondestructive tests were performed per the operating instructions of each device manufacturer. Mechanical properties were adjusted for moisture content differences per ASTM D1990-16 (ASTM 2016).

3 Testing

The specimens were subjected to both nondestructive evaluation and static bending tests. The nondestructive testing devices were Fibre-gen's Director HM200 (Fibre-gen, Christchurch, New Zealand) (hereafter Director or "dire") and Metriguard's E-computer Model 340 (Metriguard, Pullman, Washington, USA) (hereafter E-computer or "ecomp").

The Director is a handheld device that estimates MOE by measuring the acoustic velocity (in feet per second or meters per second) of a longitudinal stress wave traveling through a specimen.

For the Director test, each specimen was supported in a flatwise orientation by two sawhorses allowing approximately 1 ft (30 cm) of specimen overhang on each end. The device's sensor was held against one end of the specimen while a tap was administered to the same end with a hammer. The device generated an acoustic velocity output in feet per second from which a dynamic MOE value in pounds per square inch was calculated via $E = \rho V^2$, where E is elasticity, ρ is density, and V is acoustic velocity (Ross and Pellerin 1994). The E value was recorded for subsequent analysis.

The E-computer device estimates MOE by measuring transverse vibration. For the E-computer test, each specimen was supported near its ends by two metal tripods. One tripod was topped with a transducer connected by a cord to a laptop computer. The transducer measured the transverse vibration of the test piece. All pieces were tested in a flatwise orientation. After a specimen was weighed, its ends were aligned with the tops of the tripods allowing for a 1-in. (2.54-cm) overhang at each end. Oscillation was initiated by lightly tapping each specimen near its midpoint. The transducer sensed the vibration, and the laptop generated a dynamic MOE output recorded in pounds per square inch. The software calculates the elasticity value via the formula

$$E = f^2 \times W \times S^3/(C \times I \times g)$$

where E is modulus of elasticity, f is the frequency of the specimen's vibration, W is the weight of the specimen, S is the span, C is a constant, I is the moment of inertia, and g is the acceleration due to gravity (Ross and Pellerin 1994).

The static bending tests were performed on an Instron universal testing machine (Instron Corporation, Norwood, Massachusetts, USA) per the Flexure Test Method under ASTM D198-15 (ASTM 2015b) (Fig. 1). We refer to the MOE estimate obtained from the static bending tests as "sb MOE." The specimens were loaded in an edgewise orientation. Although third-point loading and a span-to-depth ratio of 17:1 were used (59.5 in, or 151.13 cm), the test pieces were not trimmed to this length. Instead, the specimens were placed in the fixture such that the randomly-determined span boundaries and corresponding load head placement markers lined up with the reaction supports and the load heads, respectively. Whatever overhang there was on either end was allowed to remain.

The moisture content of each piece at the time of testing was measured from its face approximately halfway between the load head markings with a Delmhorst J-88 pin-type moisture meter (Delmhorst Instrument Company, Towaco, New Jersey, USA) to a depth of approximately 8 mm. Prior to zeroing the extensometer (used to measure deflection), each specimen was loaded with approximately 222.4 N to ensure proper placement and seating of the load heads. The test was then applied until full rupture. The average length of time until rupture was approximately 5 min.

Prior to analysis, all MOR and MOE values for all tests were adjusted per ASTM D1990-16 (ASTM 2016) to a nominal moisture content of 15%. The average moisture content prior to adjustment was 13.3%.

4 Evaluation of Statistical Models for the MOE and MOR Distributions

The objective of this study was to identify (if possible) statistical distributions that yield good models for *full* MOE or MOR populations (as opposed to populations corresponding to specific visual grades or specific MSR limits). To this end, we fit various univariate distributions to the samples of 200 MOE or MOR values. These fits are discussed in Section 4.1.

We also fit mixtures of bivariate normal distributions to the samples of 200 pairs of MOE and MOR values. These fits are discussed in Section 4.2.

4.1 Univariate Models

We fit three univariate models — two-parameter Weibull, normal, and mixed normal — to each of the MOE measures. We fit five univariate models — two-parameter Weibull, normal, three-parameter beta, skew normal, and mixed normal — to the MOR values. The probability density functions of these probability distributions are provided in the Appendix.

A summary of the (maximum likelihood) parameter estimates for the univariate distributions is provided in Table 1, and a summary of our tests of the goodness-of-fit of various distributions is provided in Table 2.

The univariate normal fits and the Shapiro-Wilk test of normality were performed in the R programming environment (R Core Team, 2013). The maximum likelihood fits for the other univariate distributions and the associated Cramér-von Mises and likelihood ratio tests were performed via Fortran programs written by the authors. The source code for these programs can be found at `http://www1.fpl.fs.fed.us/mordist.html`. The Cramér-von Mises test for a two-parameter Weibull distribution is based on sections 4.10 and 4.11 of D'Agostino and Stephens (1986) and makes use of their table 4.17 to calculate critical values for the test. For the other distributions, critical values were obtained via a "parametric bootstrap" (a particular type of computer simulation — please see the source code of the programs for details).

4.1.1 Static Bending MOE ("sb MOE")

Figures 2-4 provide probability plots of two-parameter Weibull, normal, and mixed normal fits to the sb MOE data. Figure 5 provides a histogram of the sb MOE data overlaid with the fitted normal and Weibull distributions. Figure 6 provides a histogram of the sb MOE data overlaid with the fitted normal and mixed normal distributions. Figure 7 provides a histogram of the sb MOE data overlaid with the fitted mixed normal distribution and its two components.

A Cramér-von Mises test *rejects* the null hypothesis of a two-parameter Weibull with a p-value of 0.01. A Shapiro-Wilk test of normality *does not reject* the null hypothesis of a normal distribution (the p-value equals 0.37.) A likelihood ratio test *does not reject* the null hypothesis of a normal distribution versus the alternative of a mixed normal distribution (the p-value equals 0.35).

4.1.2 Dynamic MOE — E-computer ("ecomp")

Figures 8-10 provide probability plots of two-parameter Weibull, normal, and mixed normal fits to the ecomp data. Figure 11 provides a histogram of the ecomp data overlaid with the fitted normal and Weibull distributions. Figure 12 provides a histogram of the ecomp data overlaid with the fitted normal and mixed normal distributions. Figure 13 provides a histogram of the ecomp data overlaid with the fitted mixed normal distribution and its two components.

A Cramér-von Mises test *rejects* the null hypothesis of a two-parameter Weibull with a p-value of 0.01. A Shapiro-Wilk test of normality *does not reject* the null hypothesis of a normal distribution (the p-value equals 0.32.) A likelihood ratio test *does not reject* the null hypothesis of a normal distribution versus the alternative of a mixed normal distribution (the p-value equals 0.46).

4.1.3 Dynamic MOE — Director ("dire")

Figures 14-16 provide probability plots of two-parameter Weibull, normal, and mixed normal fits to the dire data. Figure 17 provides a histogram of the dire data overlaid with the fitted normal and Weibull distributions. Figure 18 provides a histogram of the dire data overlaid with the fitted

normal and mixed normal distributions. Figure 19 provides a histogram of the dire data overlaid with the fitted mixed normal distribution and its two components.

A Cramér-von Mises test *rejects* the null hypothesis of a two-parameter Weibull with a p-value of 0.01. A Shapiro-Wilk test of normality *does not reject* the null hypothesis of a normal distribution (the p-value equals 0.19.) However, a likelihood ratio test *does reject* the null hypothesis of a normal distribution versus the alternative of a mixed normal distribution (the p-value equals 0.01). A Cramér-von Mises test *does not reject* the null hypothesis of a mixed normal distribution (the p-value equals 0.67).

4.1.4 MOR

Unlike the MOE data, the MOR data were left-skewed. This led us to consider two additional distributions: a three-parameter beta and a skew normal. (See the Appendix for the probability density functions of the five distributions.)

Figures 20-24 provide probability plots of two-parameter Weibull, normal, three-parameter beta, skew normal, and mixed normal fits to the MOR data. Figure 25 provides a histogram of the MOR data overlaid with the fitted normal and Weibull distributions. Figure 26 provides a histogram of the MOR data overlaid with the fitted normal and three-parameter beta distributions. Figure 27 provides a histogram of the MOR data overlaid with the fitted skew normal distribution. Figure 28 provides a histogram of the MOR data overlaid with the fitted normal and skew normal distributions. Figure 29 provides a histogram of the MOR data overlaid with the fitted normal and mixed normal distributions. Figure 30 provides a histogram of the MOR data overlaid with the fitted mixed normal distribution and its two components.

A Cramér-von Mises test *rejects* the null hypothesis of a two-parameter Weibull at a 0.01 significance level. (An Anderson-Darling test also *rejects* the null hypothesis of a two-parameter Weibull at a 0.01 significance level.) A Shapiro-Wilk test of normality *rejects* the null hypothesis of a normal distribution at a 0.001 significance level. Also, a likelihood ratio test *rejects* the null hypothesis of a normal distribution versus the alternative of a mixed normal distribution (the p-value equals 0.0007). A Cramér-von Mises test *rejects* the null hypothesis of a three-parameter beta distribution at a 0.01 significance level. A Cramér-von Mises test *does not reject* the null hypothesis of a skew normal distribution (the p-value was 0.65). A Cramér-von Mises test *does not reject* the null hypothesis of a mixed normal distribution (the p-value was 0.66).

4.2 Bivariate Models

The models discussed in Section 4.1 are "univariate" models. That is, they are models for the distributions of single variables (sb MOE, ecomp, dire, or MOR). However, strength and stiffness are positively correlated, and there is extra information to be gained by modeling the joint behavior of sb MOE and MOR (or ecomp and MOR or dire and MOR). Our univariate work suggests that MOR might be modeled by a skew normal distribution or a mixture of two univariate normals, and sb MOE, ecomp, and dire might be modeled as normals or mixtures of two univariate normals.

It can be shown that if a bivariate stiffness-strength distribution is a mixture of bivariate normals, then the corresponding univariate (or "marginal") stiffness and strength distributions will be mixtures of univariate normals. Statisticians also know that if variables X and Y have a bivariate normal distribution, then a plot of Y versus X values will be an approximately elliptical cloud of data points. In Figures 31-33, we plot MOR versus sb MOE, MOR versus ecomp, and MOR versus dire. All three scatter plots suggest that the bivariate stiffness-strength distributions might be well-approximated by mixtures of bivariate normal distributions. To investigate this possibility we

used maximum likelihood methods to fit mixtures of two bivariate normal distributions to the sb MOE-MOR, ecomp-MOR, and dire-MOR data sets. The programs that we wrote to perform these fits can be found at `http://www1.fpl.fs.fed.us/mix_bivn_code.html`. The density of a mixture of two bivariate normal distributions is provided in the Appendix.

In Table 3 we report the parameter estimates from these fits. The lower left cloud in the appropriate MOE-MOR scatter plot (Figures 31-33) corresponds to the "Left bivariate normal" fit in Table 3. The upper right cloud corresponds to the "Right bivariate normal" fit in Table 3.

The fitted $\hat{\mu}_{\text{MOE},1}$, $\hat{\sigma}_{\text{MOE},1}$, $\hat{\rho}_1$, $\hat{\mu}_{\text{MOR},1}$, $\hat{\sigma}_{\text{MOR},1}$, $\hat{\mu}_{\text{MOE},2}$, $\hat{\sigma}_{\text{MOE},2}$, $\hat{\rho}_2$, $\hat{\mu}_{\text{MOR},2}$, $\hat{\sigma}_{\text{MOR},2}$, and $\hat{p}$ in Table 3 correspond to the parameters $\mu_{\text{X},1}$, $\sigma_{\text{X},1}$, ρ_1, $\mu_{\text{Y},1}$, $\sigma_{\text{Y},1}$, $\mu_{\text{X},2}$, $\sigma_{\text{X},2}$, ρ_2, $\mu_{\text{Y},2}$, $\sigma_{\text{Y},2}$, and p described in Section 7.6 of the Appendix. In particular, $\hat{p}$ is our estimate of the proportion of specimens that come from the lower left bivariate normal population.

The bivariate fits can be used to calculate "probability contours." For example, for a bivariate normal distribution, a 0.90 probability contour is an ellipse centered at the bivariate mean of the distribution that will (over the long run) contain 90% of (X, Y) pairs randomly drawn from the distribution. In each of Figures 34-36 we have superimposed 0.90 probability ellipses corresponding to the two bivariate normal *components* of the mixed bivariate normal distributions fitted to the sb MOE-MOR, ecomp-MOR, and dire-MOR data clouds displayed in Figures 31-33. In Figures 37-39 we plot 0.90 probability contours for the *full* mixed bivariate normal distributions. The plots do not *prove* anything, and we suspect that if we performed formal goodness-of-fit tests (difficult for mixed bivariate normals), mixed bivariate normal hypotheses might be rejected. However, the plots do lend some support to the intuition that full lumber stiffness-strength distributions will likely be mixtures of distributions. (In our case, the stiffness-strength distributions appear to be mixtures of two roughly bivariate normal distributions.)

5 Summary

Verrill *et al.* (2014, 2015) demonstrated theoretically and empirically that the MOR distribution of visually graded or MSR lumber is not a Weibull. Instead, the tails of the MOR distribution are thinned via "pseudo-truncation."

The *theoretical* portion of Verrill *et al.*'s argument was based on the assumption of a bivariate normal-Weibull (Gaussian-Weibull) MOE-MOR distribution for the *full* population of lumber (as opposed to the bivariate distribution of visual or MSR grades of lumber). We felt that it was worthwhile to investigate this assumption. In the absence of data sets in the literature that were drawn from the full population at a mill, we determined to obtain such a sample for analysis. In this paper we have reported the results from this analysis.

Our sample suggests that the full population MOR distribution is not a normal, a two-parameter Weibull, or a three-parameter beta. Skew normal and mixed normal distributions are not rejected by our analysis.

This implies that full population bivariate MOE-MOR distributions might not be Gaussian-Weibull (because full MOR populations might not be Weibull), and thus MOR distributions for MSR lumber or a visual grade might not be pseudo-truncated Weibulls. (However, the MOR distributions of MSR lumber or visual grades of lumber will still have "thinned tails.")

We have also found that full population stiffness values (sb MOE, ecomp, and dire) are not distributed as two-parameter Weibulls. Analyses of the sb MOE and ecomp data suggest that the distributions of these two variables might be well-approximated by normals. Analysis of the dire data rejects a normal distribution. A mixed normal distribution is not rejected for any of the three stiffness measures.

We *strongly* emphasize that we do not mean to conclude on the basis of a single sample of size 200 from the full MOE-MOR 2x4 lumber population produced during a single day at a single mill that full population MOEs are normal or mixed normal and full population MORs are skew normal or mixed normal. From the current experiment, we *do* mean to conclude that if reliability engineers are entertaining the idea of obtaining new efficiencies via careful probability modeling of strength properties, additional experimental research must be done on the fundamental question of valid models for stiffness and strength distributions for full populations of lumber from a single mill on a single day. (These "full" distributions are then subject to pseudo-truncation in the formation of visual or MSR grades.) Further, we suspect that even if research determines that a simple model can characterize such a distribution, further research will determine that this simple model varies from day to day, mill to mill, and region to region so that an ever-changing mixture model is the correct model. In this case, designers of new and complex wood structural products would need to assure themselves that their reliability models are robust to incorrect lumber strength and stiffness assumptions.

We intend to perform additional empirical investigations and fits to the resulting samples to form part of the foundation for such reliability models. However, such studies are expensive, and given the fact that we expect that actual distributions may be complicated mixtures of base distributions that vary from mill to mill, region to region, time to time, size to size, and species to species, it may be that no satisfactory theoretical form(s) can be identified to form the basis of sophisticated reliability models that would yield an increase in overly conservative design values.

We suspect that ultimately, if reliability engineers want to obtain accurate reliability estimates, they will need to develop detailed computer models that yield real-time, in-line estimates of lumber strength based on measurements of stiffness, specific gravity, knot size and location, slope of grain, and other strength predictors.

Acknowledgments

The authors acknowledge and thank the Southern Pine Inspection Bureau for their gracious contributions to this research. The authors also thank Dr. Jim Baldwin of the USDA Forest Service Pacific Southwest Research Station for suggesting Figures 37-39 and for providing R code that could be used to create such figures.

6 References

ASTM (2010). Standard practice for evaluating allowable properties for grades of structural lumber, D2915-10, *Annual Book of ASTM Standards*, ASTM International, West Conshohocken, PA.

ASTM (2015a). Standard specification for computing reference resistence of wood-based materials and structural connections for load and resistance factor design, D5457-15, *Annual Book of ASTM Standards*, ASTM International, West Conshohocken, PA.

ASTM (2015b). Standard test methods of static tests of lumber in structural sizes, D198-15, *Annual Book of ASTM Standards*, ASTM International, West Conshohocken, PA.

ASTM (2016). Standard practice for establishing allowable properties for visually-graded dimension lumber from in-grade tests of full-size specimens, D1990-16, *Annual Book of ASTM Standards*, ASTM International, West Conshohocken, PA.

D'Agostino, R.B. and Stephens, M.A. (1986). Goodness-of-fit Techniques. Marcel Dekker, New York.

Evans, J.W., Johnson, R.A., and Green, D.W. (1997). "Goodness-of-fit tests for two-parameter and three-parameter Weibull distributions," Chapter 9 of *Advances in the theory and practice of statistics: A volume in honor of Samuel Kotz*, New York, NY: John Wiley & Sons, Inc., pages 159-178.

Green, D.W. and Evans, J.W. (1987). *Mechanical properties of visually graded lumber: Volumes 1-8*, Department of Commerce, National Technical Information Service, Springfield, VA, 3515 pages.

Ross, R.J. and Pellerin, R.F. (1994). "Nondestructive testing for assessing wood members in structures: A review." General Technical Report FPL-GTR-70. Madison, WI: U.S. Department of Agriculture, Forest Service, Forest Products Laboratory. 40 p.

R Core Team (2013). R: A language and environment for statistical computing. R Foundation for Statistical Computing, Vienna, Austria. URL http://www.R-project.org

Verrill, S.P., Evans, J.W., Kretschman, D.E., and Hatfield, C.A. (2014). "Reliability Implications in Wood Systems of a Bivariate Gaussian–Weibull Distribution and the Associated Univariate Pseudo-truncated Weibull." *ASTM Journal of Testing and Evaluation*, **42**, Number 2, pages 412-419.

Verrill, S.P., Evans, J.W., Kretschman, D.E., and Hatfield, C.A. (2015). "Asymptotically Efficient Estimation of a Bivariate Gaussian–Weibull Distribution and an Introduction to the Associated Pseudo-truncated Weibull." *Communications in Statistics – Theory and Methods*, **44**, pages 2957-2975.

7 Appendix — Probability Density Functions of the Distributions

7.1 Normal (Univariate Distribution)

The normal probability density function (pdf) is given by

$$f(x;\mu,\sigma) = \frac{1}{\sqrt{2\pi}}\frac{1}{\sigma}\exp\left(-(x-\mu)^2/(2\sigma^2)\right)$$

for $x \in (-\infty,\infty)$ where μ is the mean and σ is the standard deviation of the distribution. This distribution is denoted by the notation $\mathrm{N}(\mu,\sigma^2)$.

7.2 Mixed Normal (Univariate Distribution)

In this paper, when we discuss a "mixed normal distribution," we are referring to a mixture of *two* normals. Such a mixture results when specimens are drawn with probability p from a $\mathrm{N}(\mu_1,\sigma_1^2)$ distribution and with probability $1-p$ from a $\mathrm{N}(\mu_2,\sigma_2^2)$ distribution. In this case the pdf is given by

$$\begin{aligned} f(x;\mu_1,\sigma_1,p,\mu_2,\sigma_2) &= p \times \frac{1}{\sqrt{2\pi}}\frac{1}{\sigma_1}\exp\left(-(x-\mu_1)^2/(2\sigma_1^2)\right) \\ &+ (1-p) \times \frac{1}{\sqrt{2\pi}}\frac{1}{\sigma_2}\exp\left(-(x-\mu_2)^2/(2\sigma_2^2)\right) \end{aligned}$$

for $x \in (-\infty,\infty)$.

7.3 Two-parameter Weibull (Univariate Distribution)

The two-parameter Weibull has probability density function

$$f(w;\gamma,\beta) = \gamma^{\beta}\beta w^{\beta-1}\exp\left(-(\gamma w)^{\beta}\right)$$

for $w \in [0,\infty)$ where β is the shape parameter and γ is the inverse of the scale parameter.

7.4 Three-parameter Beta (Univariate Distribution)

The three-parameter beta has probability density function

$$f(x;\alpha,\beta,R) = \frac{x^{\alpha-1}(R-x)^{\beta-1}}{R^{\alpha+\beta-1}} \times \frac{\Gamma(\alpha+\beta)}{\Gamma(\alpha)\Gamma(\beta)}$$

for $x \in [0,R]$, where Γ denotes the gamma function.

7.5 Skew Normal (Univariate Distribution)

The skew normal distribution has probability density function

$$f(x;\xi,\omega,\alpha) = \frac{2}{\omega} \times \phi\left(\frac{x-\xi}{\omega}\right) \times \Phi\left(\alpha\left(\frac{x-\xi}{\omega}\right)\right)$$

for $x \in (-\infty,\infty)$, where ϕ denotes the probability density function of a standardized normal, Φ denotes the cumulative distribution function of a standardized normal, and ξ, ω, and α are the parameters of the skew normal distribution.

7.6 Mixture of Two Bivariate Normals (Bivariate Distribution)

The probability density function of a *single* bivariate normal with mean vector

$$\begin{pmatrix} \mu_X \\ \mu_Y \end{pmatrix}$$

standard deviation vector

$$\begin{pmatrix} \sigma_X \\ \sigma_Y \end{pmatrix}$$

and correlation ρ is given by

$$f\left(x,y;\begin{pmatrix} \mu_X \\ \sigma_X \\ \mu_Y \\ \sigma_Y \\ \rho \end{pmatrix}\right) = \frac{1}{2\pi}\frac{1}{\sigma_X\sigma_Y\sqrt{1-\rho^2}}\exp\left(-\arg/\left(2\left(1-\rho^2\right)\right)\right)$$

for $x, y \in (-\infty,\infty)$, where

$$\arg = \left(\frac{x-\mu_X}{\sigma_X}\right)^2 - 2\rho\left(\frac{x-\mu_X}{\sigma_X}\right)\left(\frac{y-\mu_Y}{\sigma_Y}\right) + \left(\frac{y-\mu_Y}{\sigma_Y}\right)^2$$

The probability density function of a *mixture* of two bivariate normals with first distribution proportion p is given by

$$
\begin{aligned}
g\left(x, y; \begin{pmatrix} \mu_{X,1} \\ \sigma_{X,1} \\ \mu_{Y,1} \\ \sigma_{Y,1} \\ \rho_1 \end{pmatrix}, \begin{pmatrix} \mu_{X,2} \\ \sigma_{X,2} \\ \mu_{Y,2} \\ \sigma_{Y,2} \\ \rho_2 \end{pmatrix}, p\right) &= p \times f\left(x, y; \begin{pmatrix} \mu_{X,1} \\ \sigma_{X,1} \\ \mu_{Y,1} \\ \sigma_{Y,1} \\ \rho_1 \end{pmatrix}\right) \\
&\quad + (1-p) \times f\left(x, y; \begin{pmatrix} \mu_{X,2} \\ \sigma_{X,2} \\ \mu_{Y,2} \\ \sigma_{Y,2} \\ \rho_2 \end{pmatrix}\right)
\end{aligned}
$$

	Normal		Weibull		3-parameter Beta			Skew normal		
	$\hat{\mu}$	$\hat{\sigma}$	$\hat{\lambda} = 1/\hat{\gamma}$	$\hat{\beta}$	$\hat{\alpha}$	$\hat{\beta}$	$\hat{R}$	$\hat{\xi}$	$\hat{\omega}$	$\hat{\alpha}$
sb MOE	1.42	0.35	1.56	4.45	—	—	—	—	—	—
ecomp	1.62	0.37	1.77	4.74	—	—	—	—	—	—
dire	1.57	0.36	1.71	4.74	—	—	—	—	—	—
MOR	7850	2384	8680	3.80	4.35	3.91	14800	10500	3540	-2.46

Table 1a: Parameter estimates from univariate fits — normal, two-parameter Weibull, three-parameter beta, and skew normal distributions. "sb MOE" denotes static bending MOE, "ecomp" denotes E-computer MOE, and "dire" denotes Director MOE. The MOE fits were done to MOE data in pounds per square inch divided by 1,000,000. The MOR fits were done to MOR data in pounds per square inch.

	Mixed Normal				
	$\hat{\mu}_1$	$\hat{\sigma}_1$	$\hat{p}$	$\hat{\mu}_2$	$\hat{\sigma}_2$
sb MOE	1.34	0.29	0.85	1.91	0.21
ecomp	1.53	0.20	0.23	1.65	0.40
dire	1.46	0.08	0.17	1.60	0.39
MOR/1000	6.96	2.59	0.59	9.13	1.21

Table 1b: Parameter estimates from univariate mixed normal fits. "sb MOE" denotes static bending MOE, "ecomp" denotes E-computer MOE, and "dire" denotes Director MOE. The MOE fits were done to MOE data in pounds per square inch divided by 1,000,000. The MOR fit was done to MOR data in pounds per square inch divided by 1,000.

Variable	Distribution	Tests		
		S-W	CVM	LR
sb MOE	Weibull	—	0.01	—
	Normal	0.371	—	0.351
	Mixed normal	—	—	—
ecomp	Weibull	—	0.01	—
	Normal	0.318	—	0.463
	Mixed normal	—	—	—
dire	Weibull	—	0.01	—
	Normal	0.185	—	0.012
	Mixed normal	—	0.67	—
MOR	Weibull	—	0.01	—
	3-par Beta	—	0.01	—
	Skew normal	—	0.65	—
	Normal	0.001	—	0.0007
	Mixed normal	—	0.66	—

Table 2: p-values. "S-W" denotes a Shapiro-Wilk goodness-of-fit test for normality. "CVM" denotes a Cramér-von Mises goodness-of-fit test for a distribution. "LR" denotes a likelihood ratio test of the null hypothesis that a distribution is a normal distribution versus the alternative that the distribution is a mixture of two normal distributions. "sb MOE" denotes static bending MOE, "ecomp" denotes E-computer MOE, and "dire" denotes Director MOE. Note that the 0.01 and 0.001 values in the table are not exact. The exact values could be smaller.

MOE	Left bivariate normal					Right bivariate normal					
	$\hat{\mu}_{\text{MOE},1}$	$\hat{\sigma}_{\text{MOE},1}$	$\hat{\rho}_1$	$\hat{\mu}_{\text{MOR},1}$	$\hat{\sigma}_{\text{MOR},1}$	$\hat{\mu}_{\text{MOE},2}$	$\hat{\sigma}_{\text{MOE},2}$	$\hat{\rho}_2$	$\hat{\mu}_{\text{MOR},2}$	$\hat{\sigma}_{\text{MOR},2}$	$\hat{p}$
sb MOE	1.26	0.28	0.54	6.68	2.40	1.63	0.32	0.79	9.29	1.35	0.55
ecomp	1.46	0.29	0.39	6.49	2.40	1.79	0.37	0.65	9.23	1.36	0.51
dire	1.41	0.28	0.45	6.68	2.45	1.76	0.35	0.63	9.25	1.32	0.55

Table 3: Parameter estimates from mixed bivariate normal fits. "sb MOE" denotes static bending MOE, "ecomp" denotes E-computer MOE, and "dire" denotes Director MOE. The MOE data were in pounds per square inch divided by 1,000,000. The MOR data were in pounds per square inch divided by 1,000.

Figure 1: Third-point loading fixture.

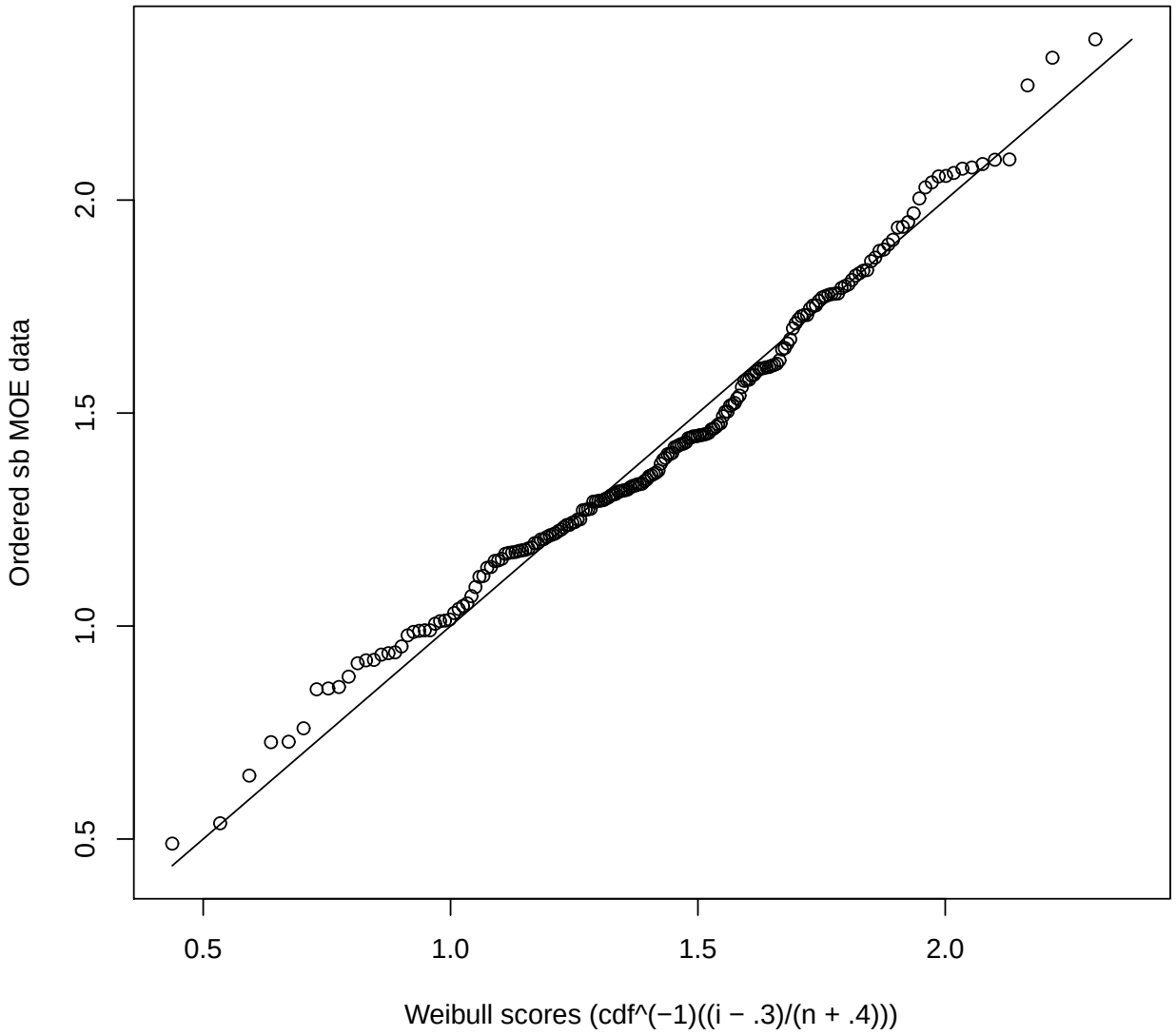

Figure 2: sb MOE. Ordered data versus predicted ordered data under the best fit Weibull model. The solid line is the $y = x$ line. If a Weibull model is appropriate, the plotted data points will lie approximately lie along the $y = x$ line.

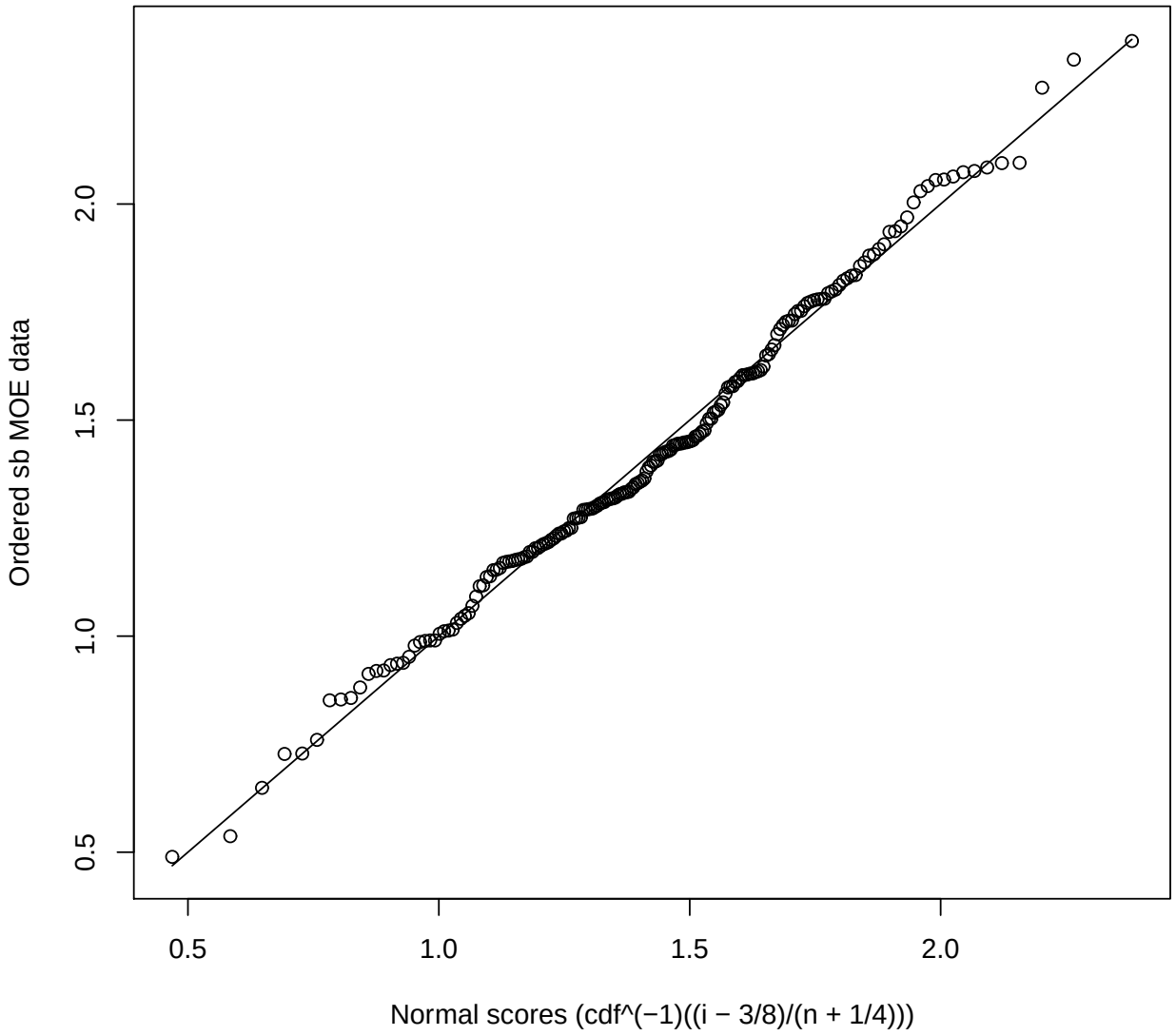

Figure 3: sb MOE. Ordered data versus predicted ordered data under the best fit normal model. The solid line is the $y = x$ line. If a normal model is appropriate, the plotted data points will lie approximately lie along the $y = x$ line.

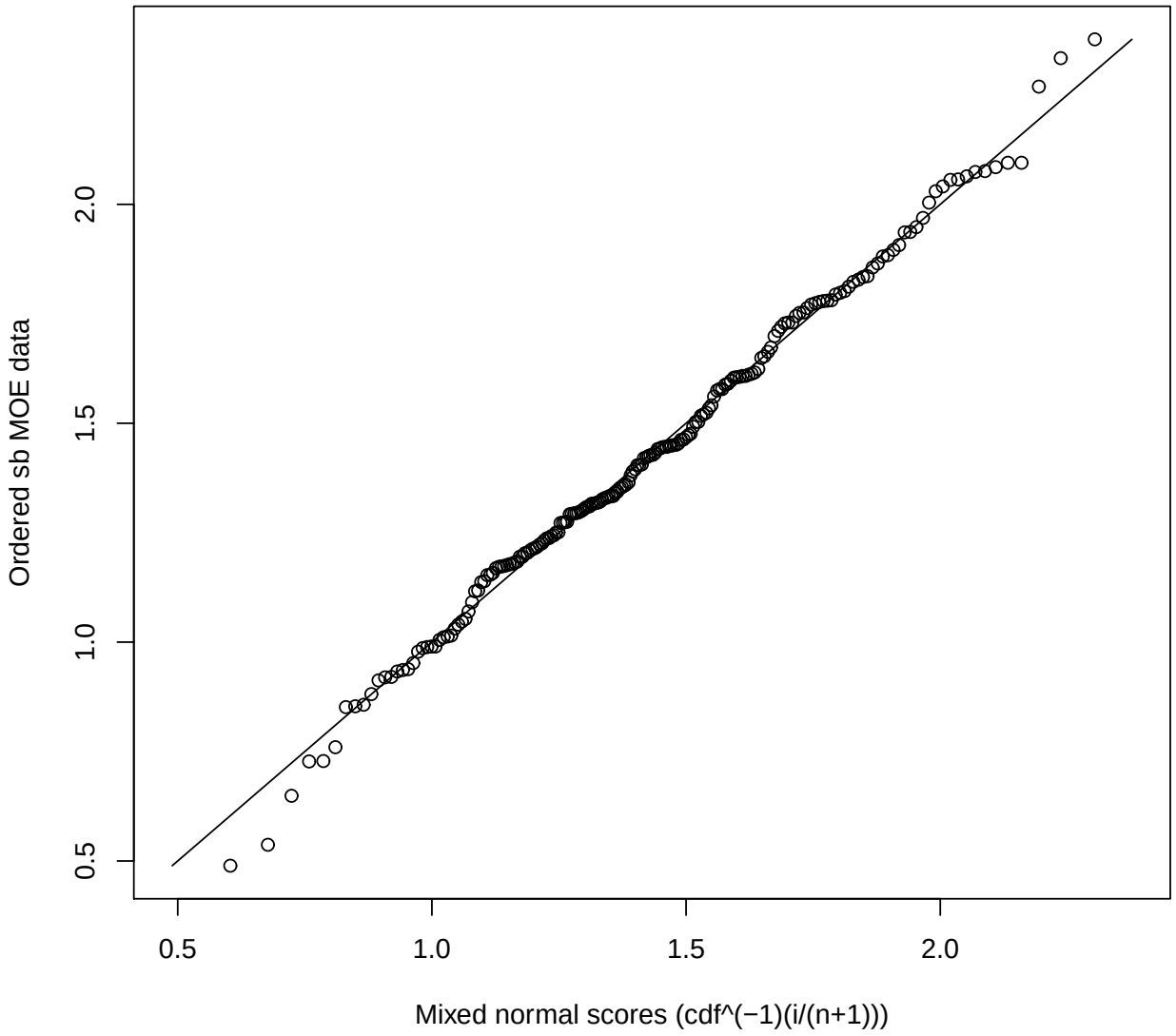

Figure 4: sb MOE. Ordered data versus predicted ordered data under the best fit mixed normal model. The solid line is the $y = x$ line. If a mixed normal model is appropriate, the plotted data points will lie approximately lie along the $y = x$ line.

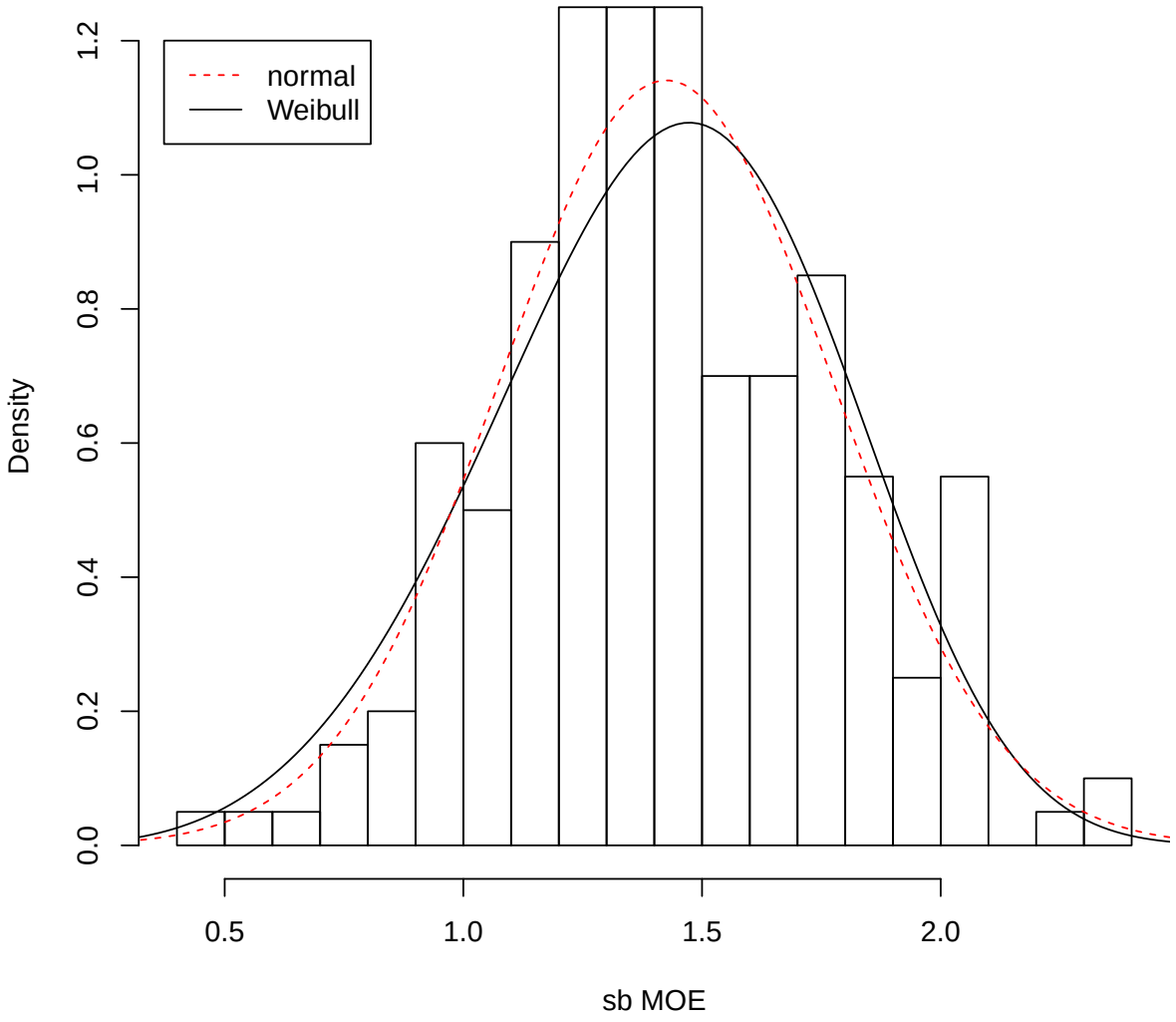

Figure 5: Histogram of the sb MOE data overlaid with the fitted normal and Weibull probability density functions.

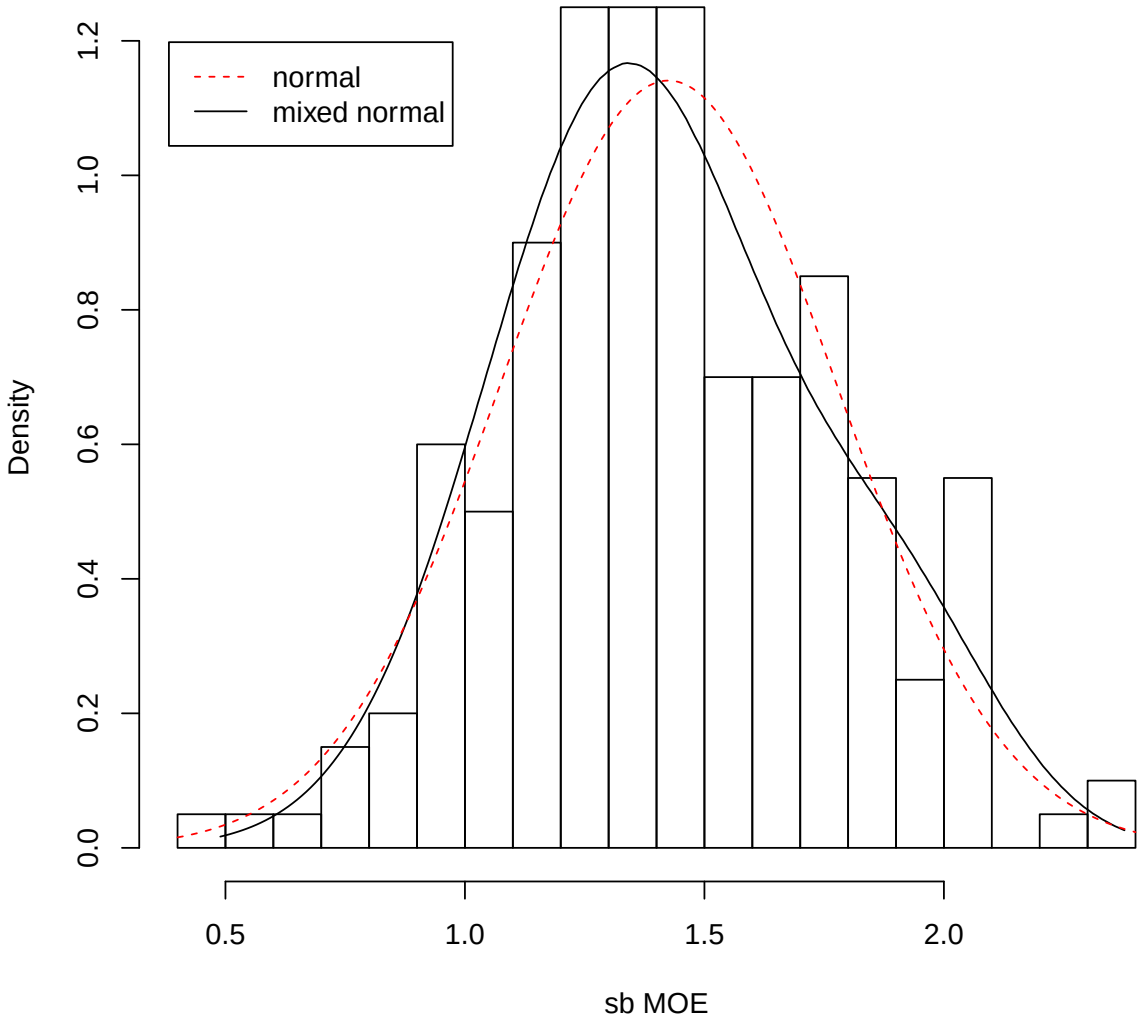

Figure 6: Histogram of the sb MOE data overlaid with the fitted normal and mixed normal probability density functions.

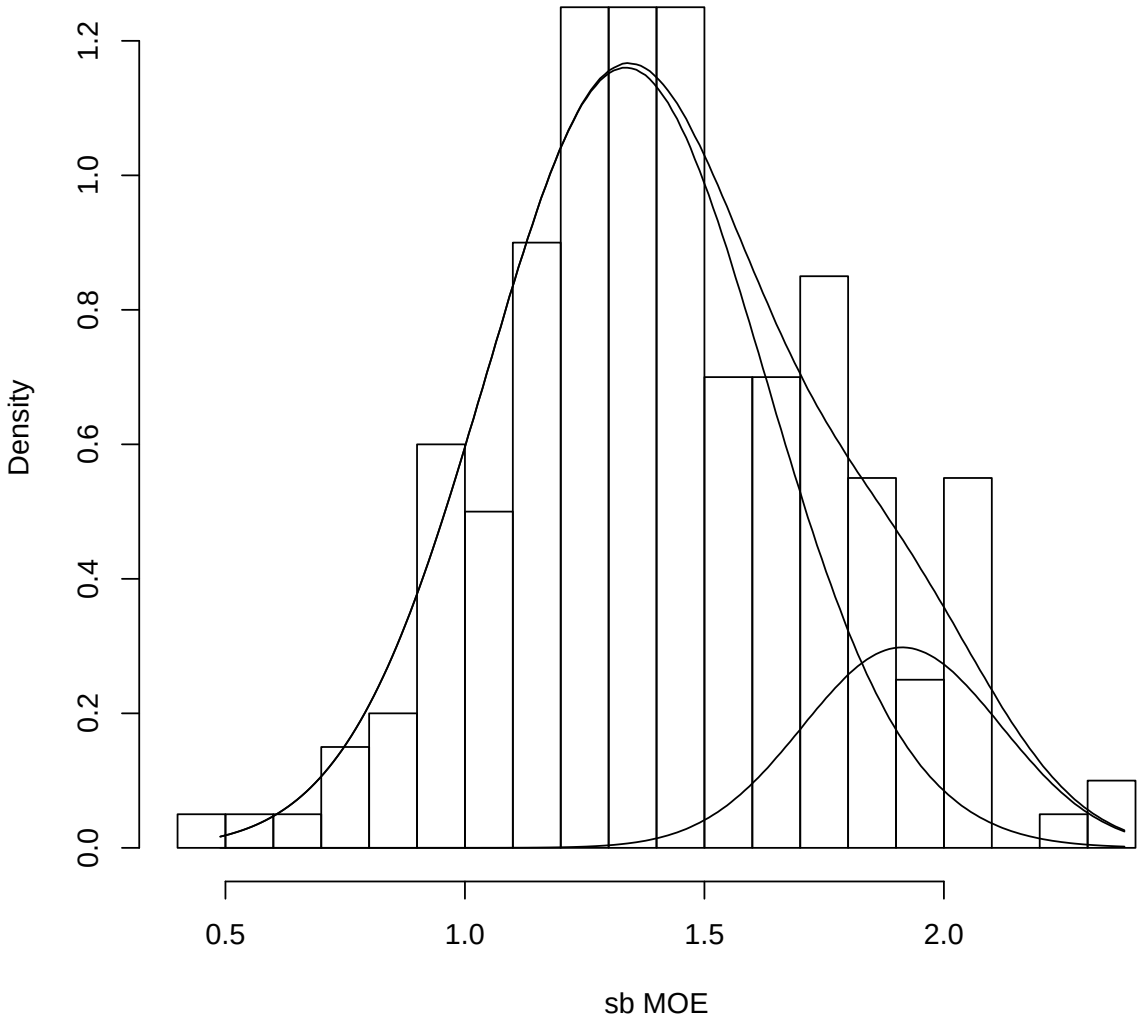

Figure 7: Histogram of the sb MOE data overlaid with the fitted mixed normal probability density function and its two components.

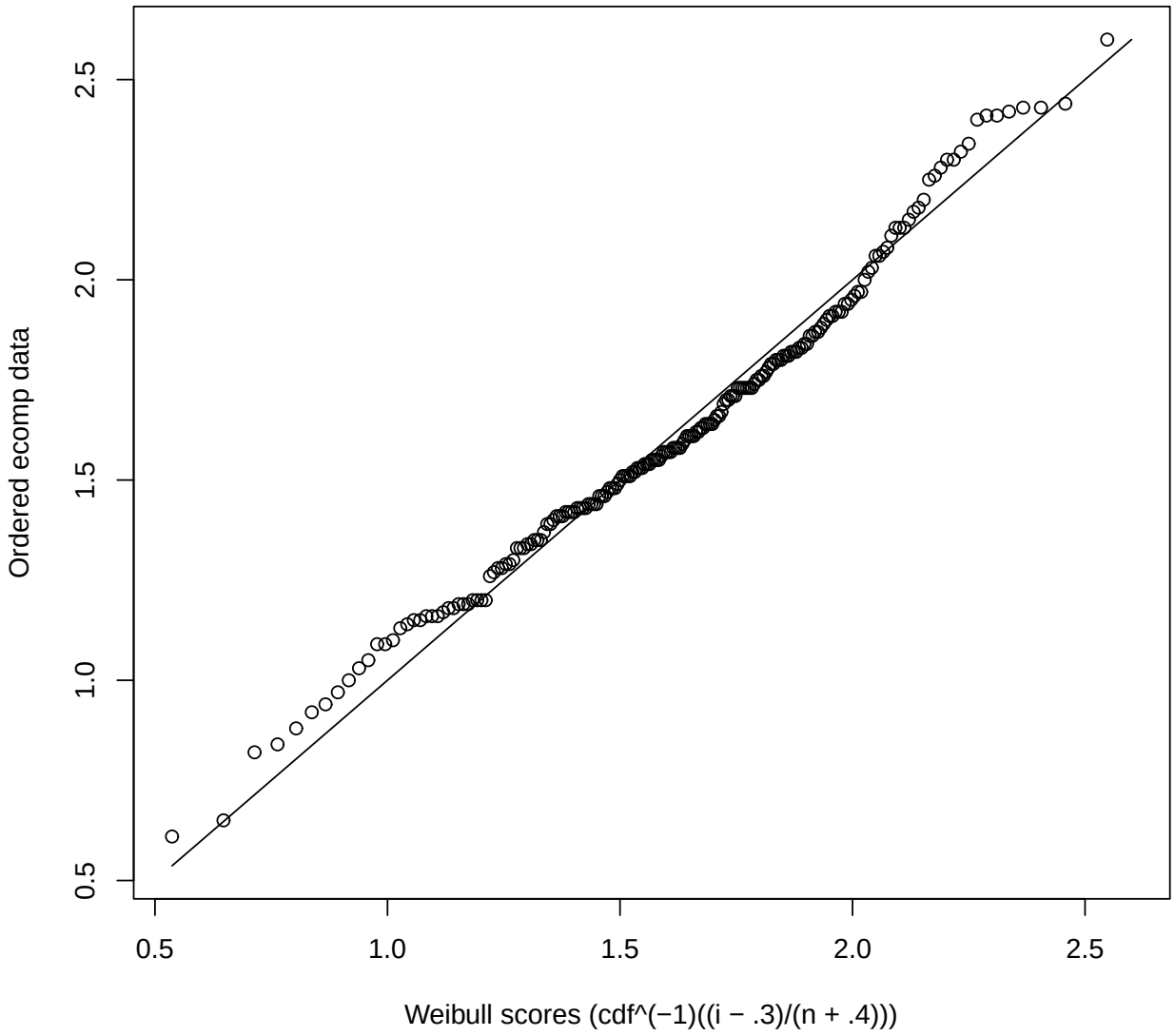

Figure 8: ecomp. Ordered data versus predicted ordered data under the fitted Weibull model. The solid line is the $y = x$ line. If a Weibull model is appropriate, the plotted data points will lie approximately along the $y = x$ line.

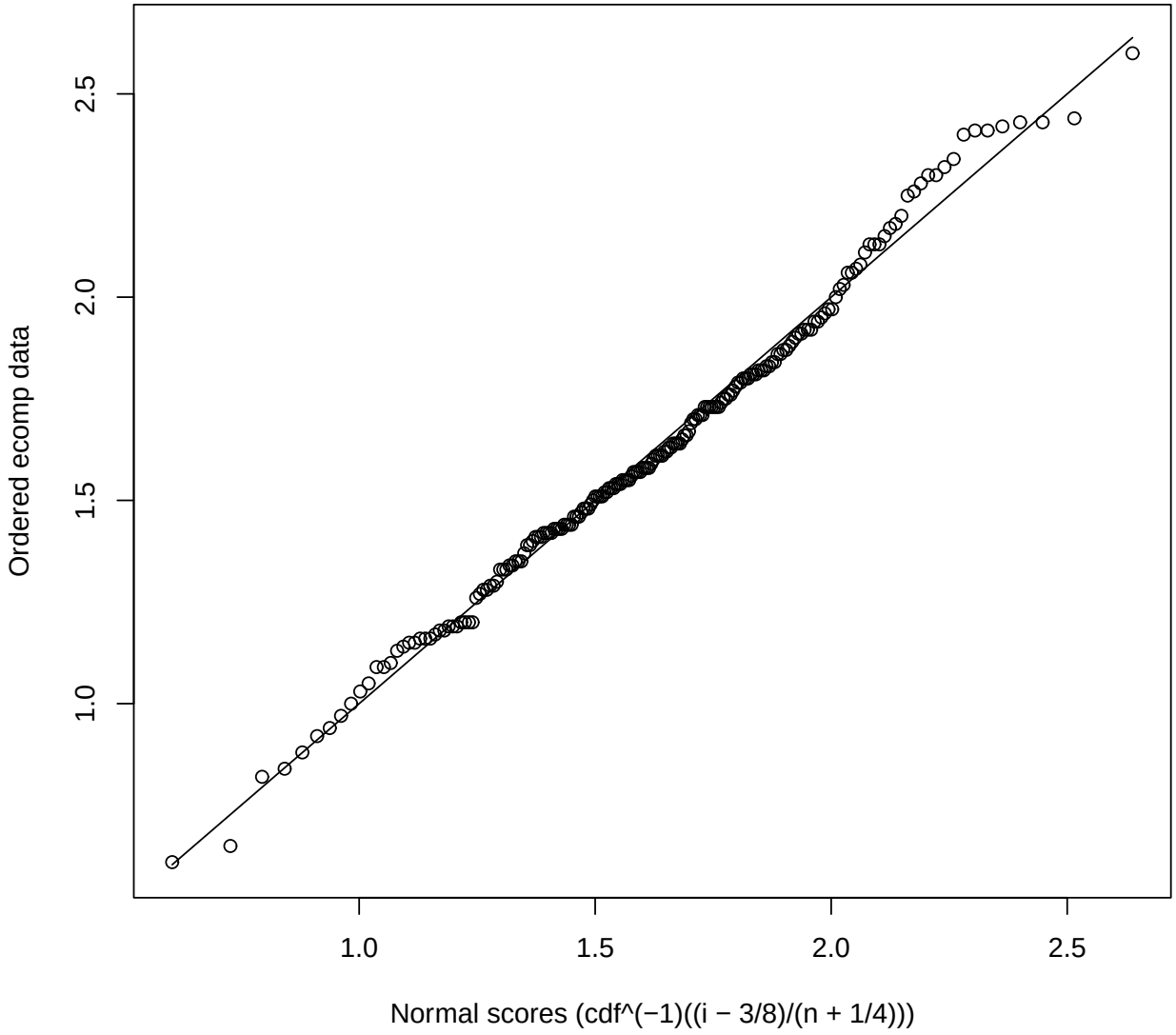

Figure 9: ecomp. Ordered data versus predicted ordered data under the fitted normal model. The solid line is the $y = x$ line. If a normal model is appropriate, the plotted data points will lie approximately along the $y = x$ line.

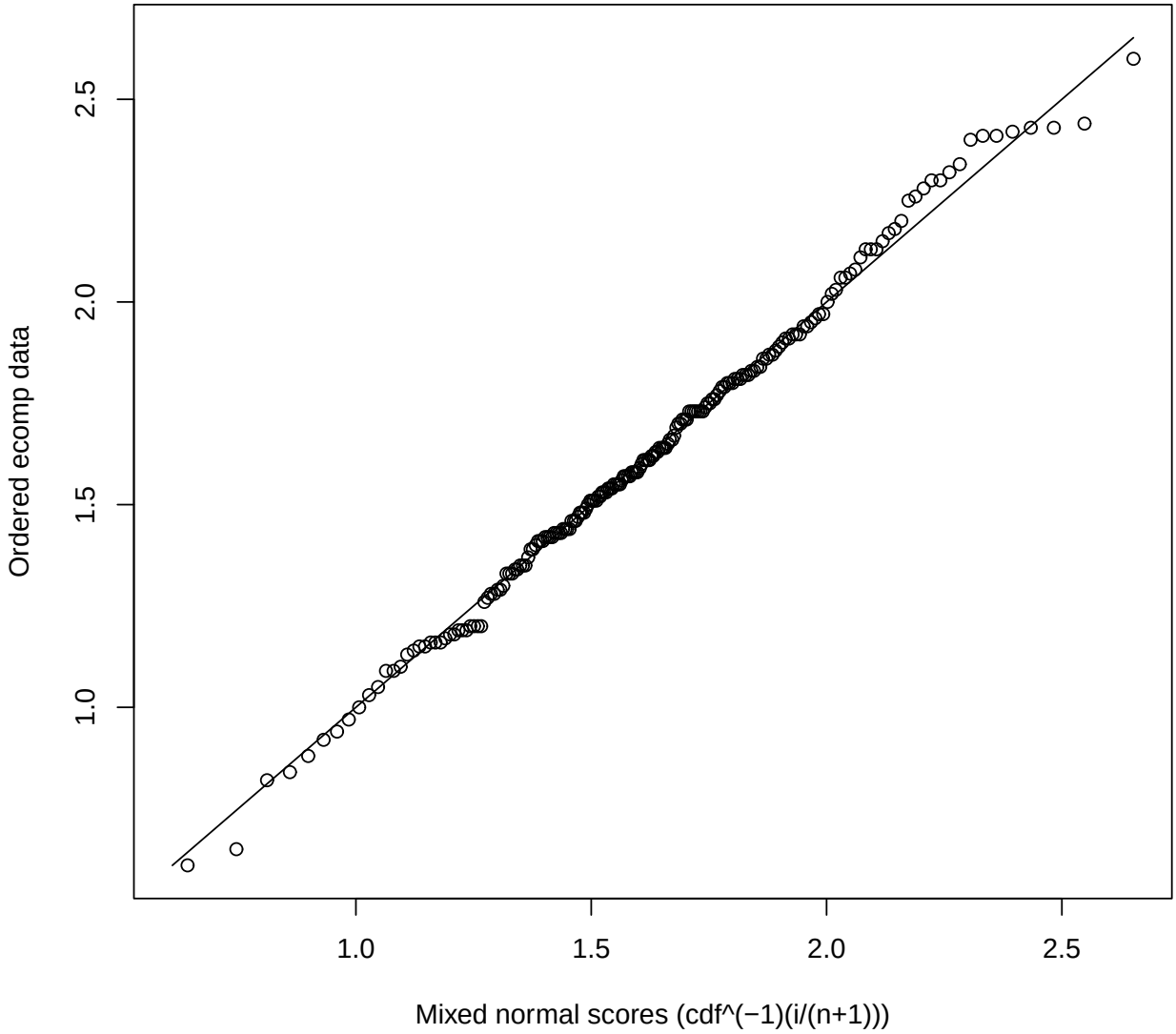

Figure 10: ecomp. Ordered data versus predicted ordered data under the fitted mixed normal model. The solid line is the $y = x$ line. If a mixed normal model is appropriate, the plotted data points will lie approximately along the $y = x$ line.

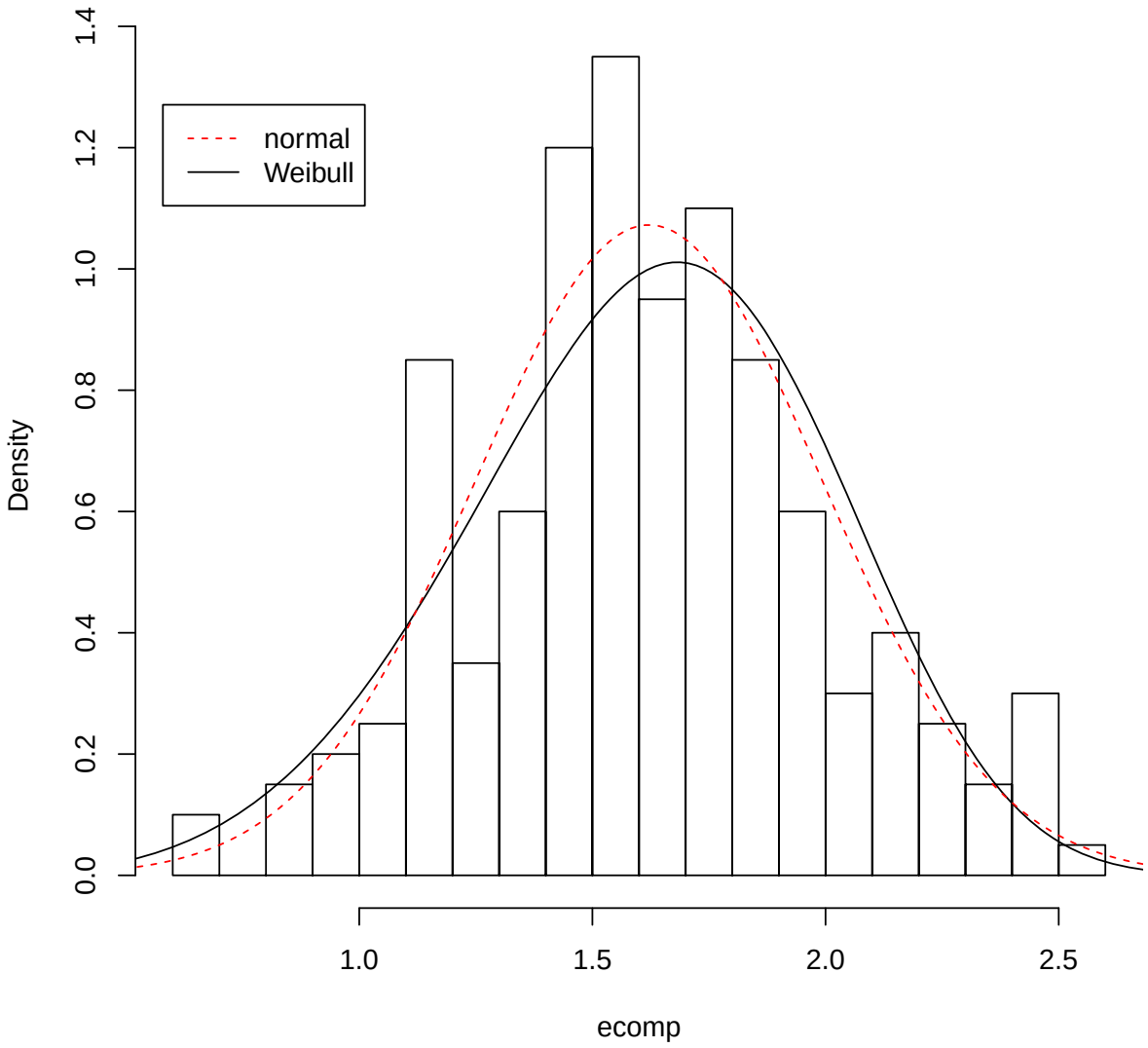

Figure 11: Histogram of the ecomp data overlaid with the fitted normal and Weibull probability density functions.

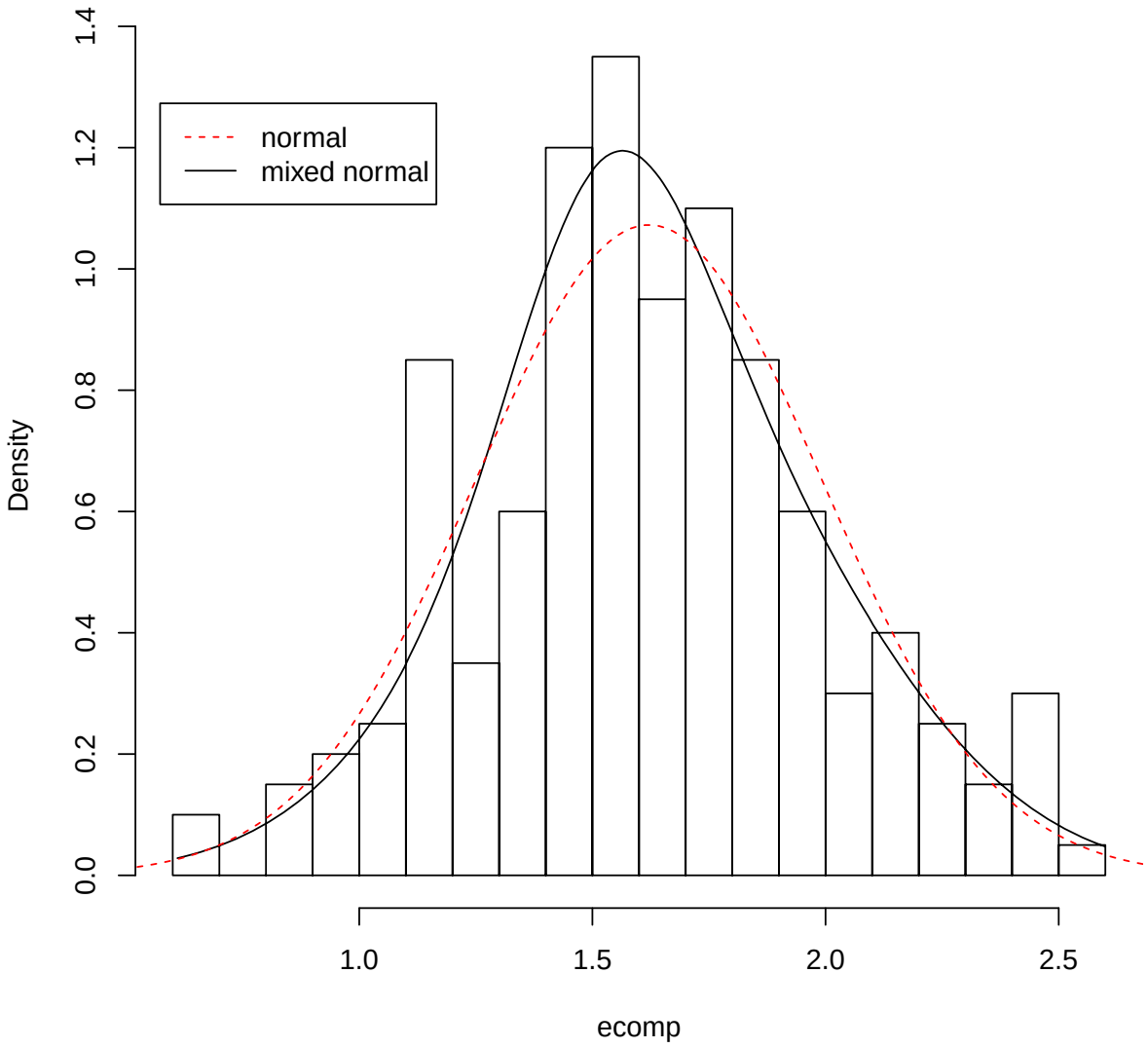

Figure 12: Histogram of the ecomp data overlaid with the fitted normal and mixed normal probability density functions.

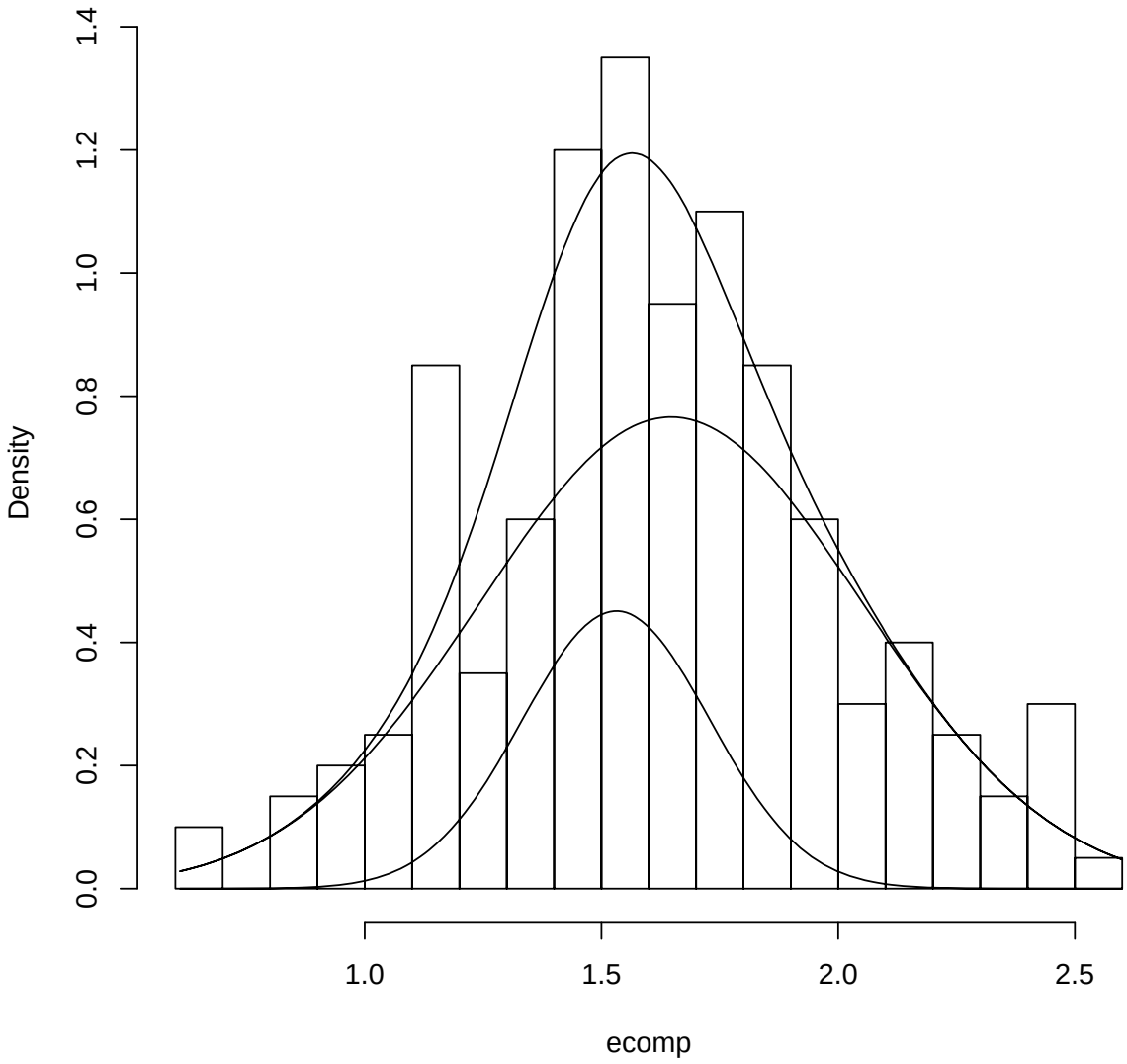

Figure 13: Histogram of the ecomp data overlaid with the fitted mixed normal probability density function and its two components.

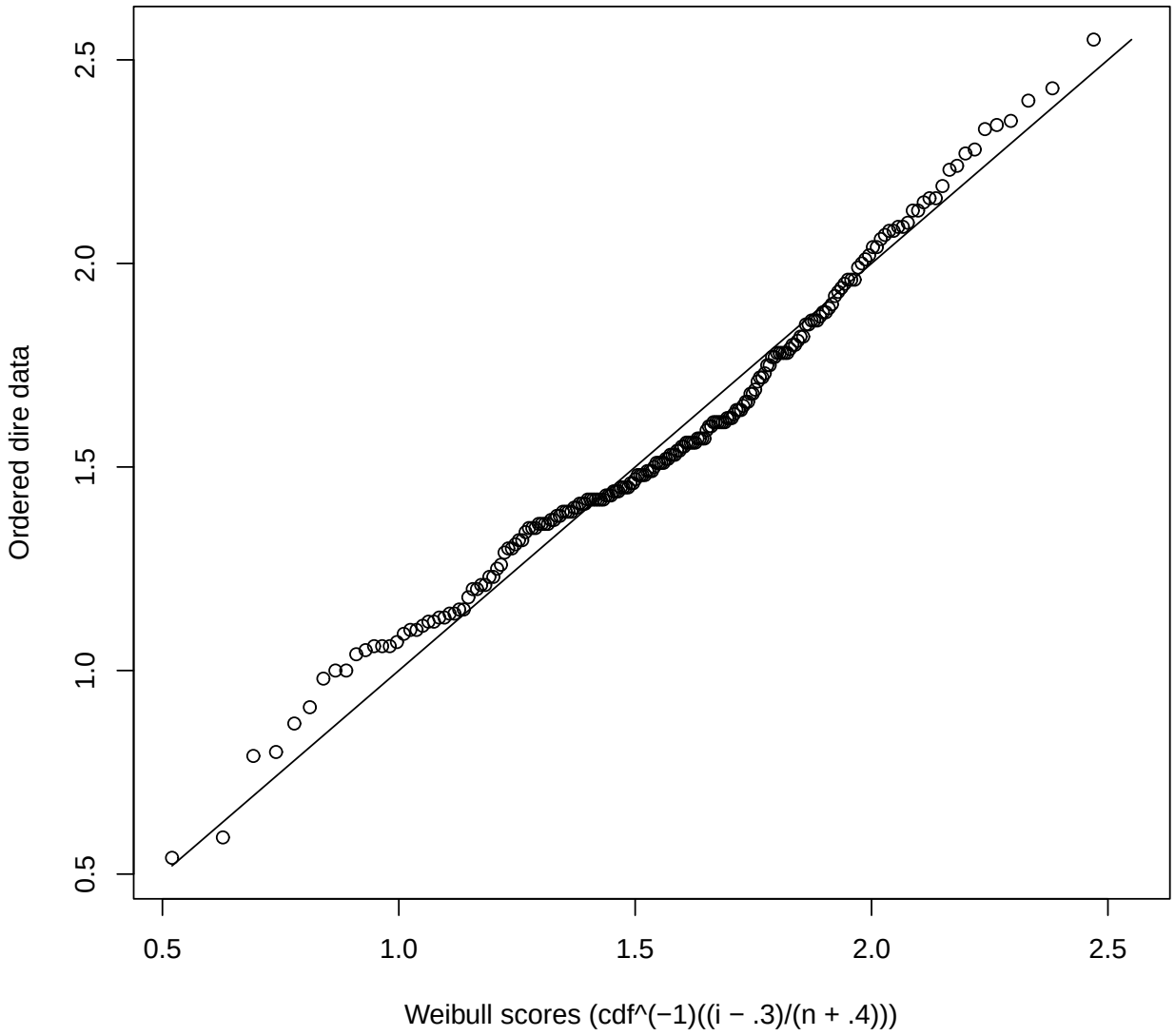

Figure 14: dire. Ordered data versus predicted ordered data under the fitted Weibull model. The solid line is the $y = x$ line. If a Weibull model is appropriate, the plotted data points will lie approximately along the $y = x$ line.

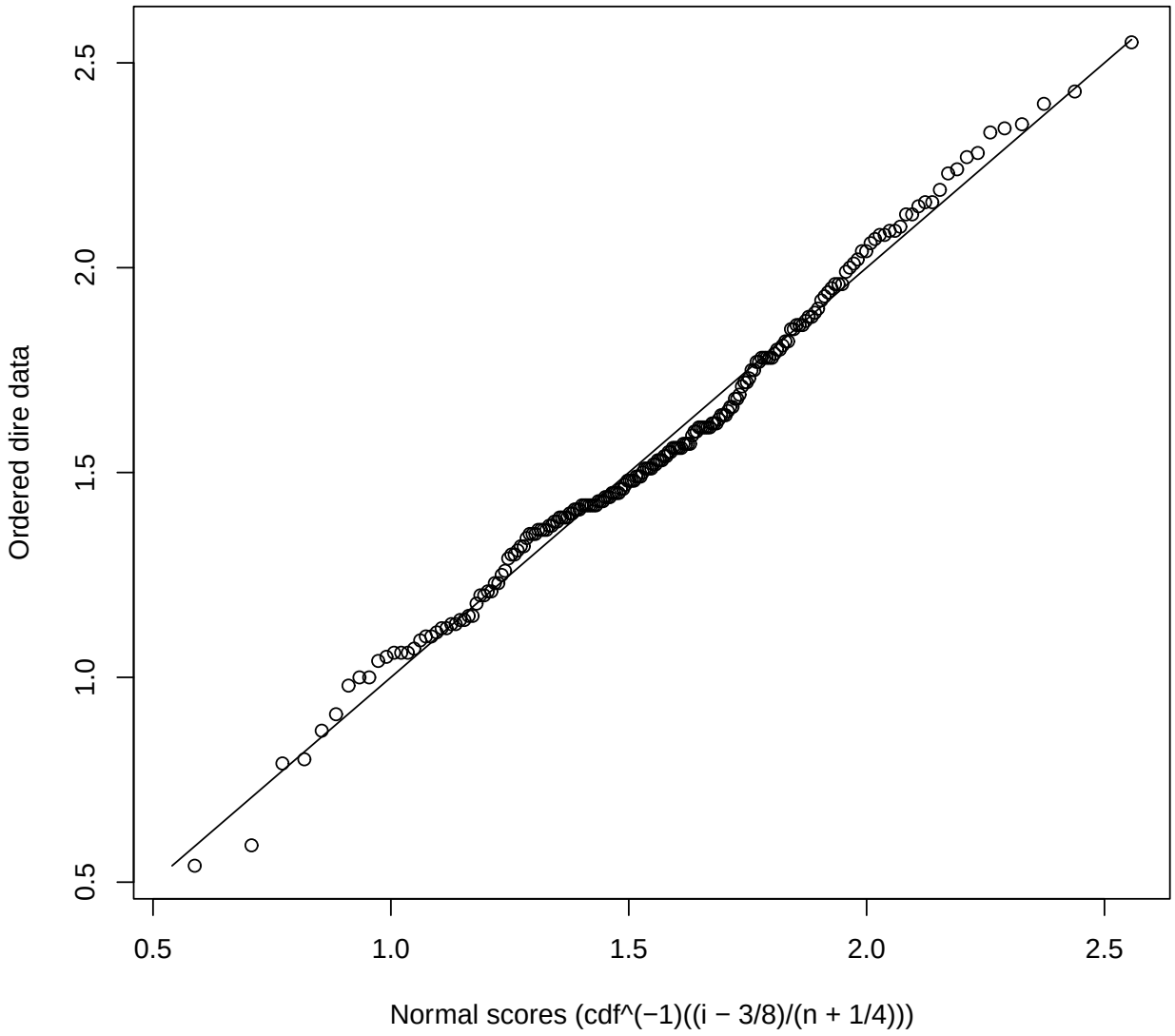

Figure 15: dire. Ordered data versus predicted ordered data under the fitted normal model. The solid line is the $y = x$ line. If a normal model is appropriate, the plotted data points will lie approximately along the $y = x$ line.

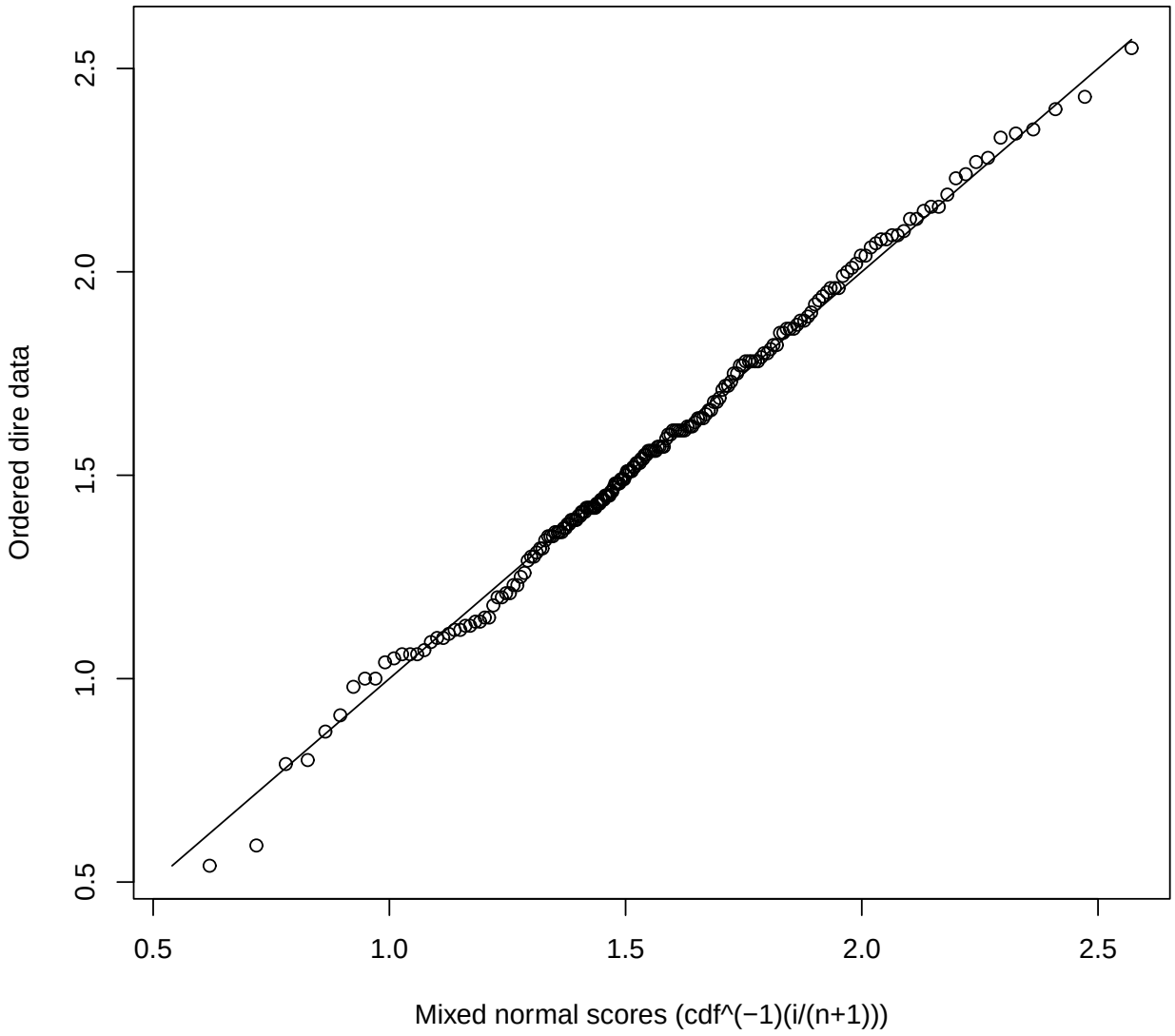

Figure 16: dire. Ordered data versus predicted ordered data under the fitted mixed normal model. The solid line is the $y = x$ line. If a mixed normal model is appropriate, the plotted data points will lie approximately along the $y = x$ line.

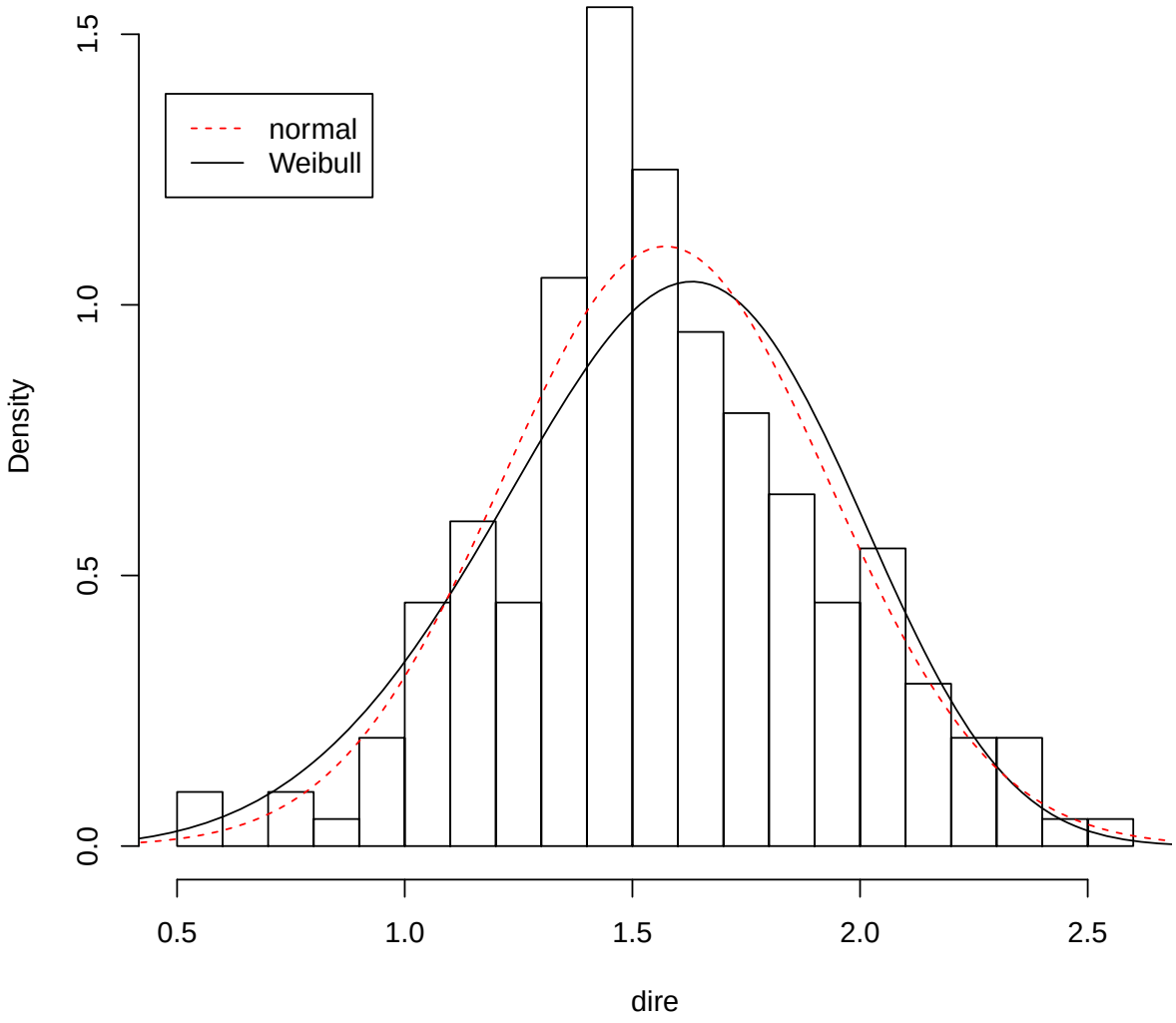

Figure 17: Histogram of the dire data overlaid with the fitted normal and Weibull probability density functions.

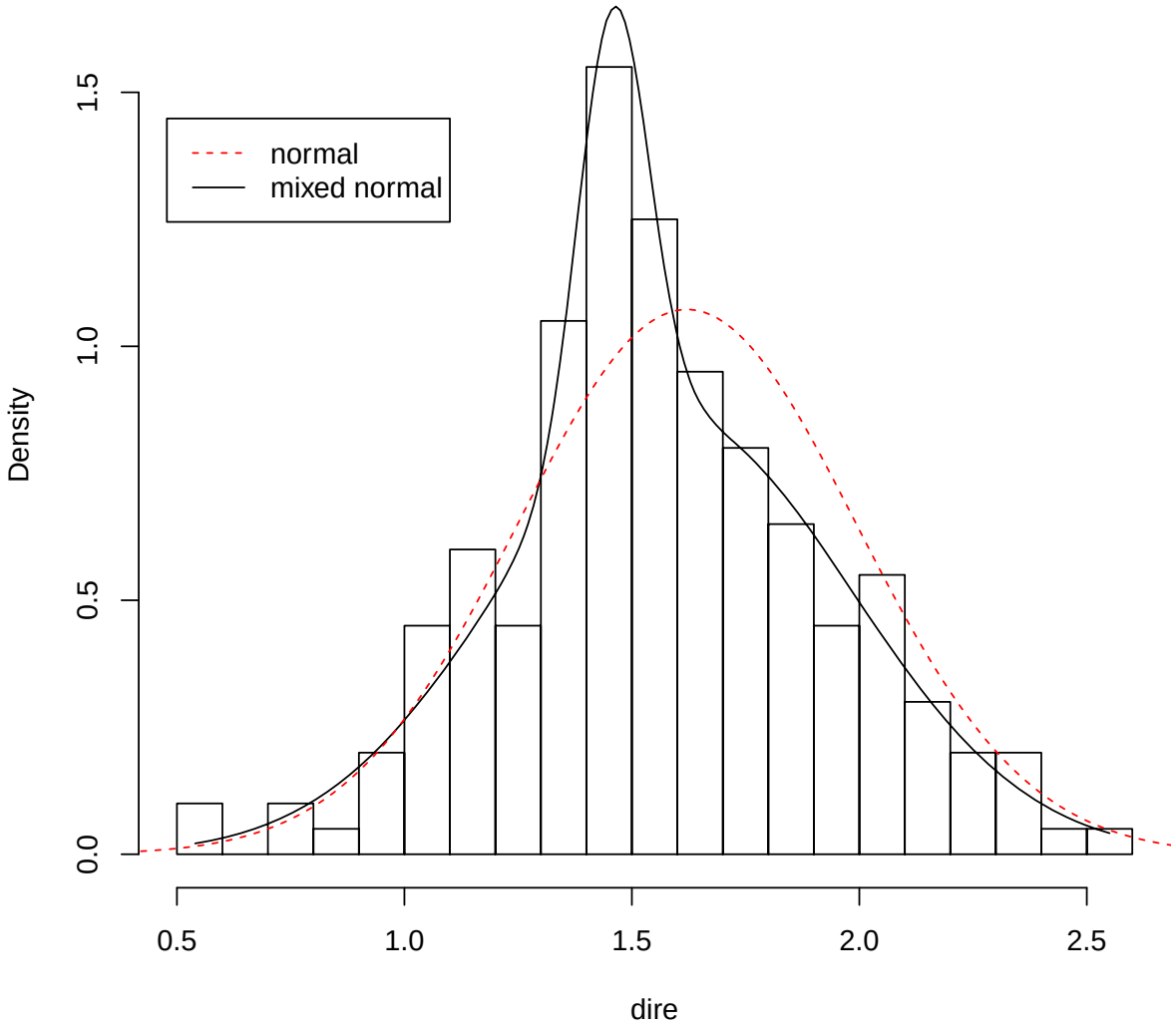

Figure 18: Histogram of the dire data overlaid with the fitted normal and mixed normal probability density functions.

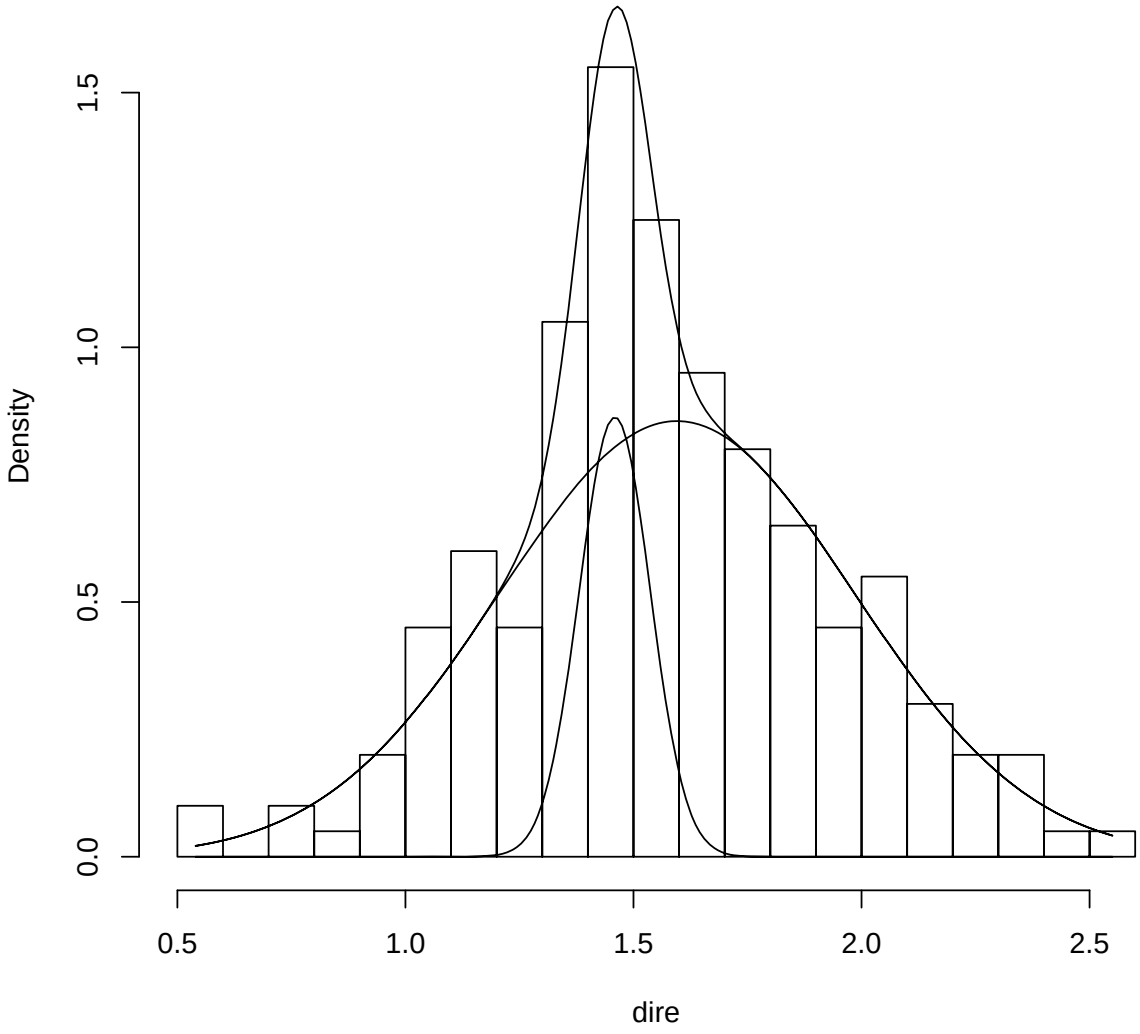

Figure 19: Histogram of the dire data overlaid with the fitted mixed normal probability density function and its two components.

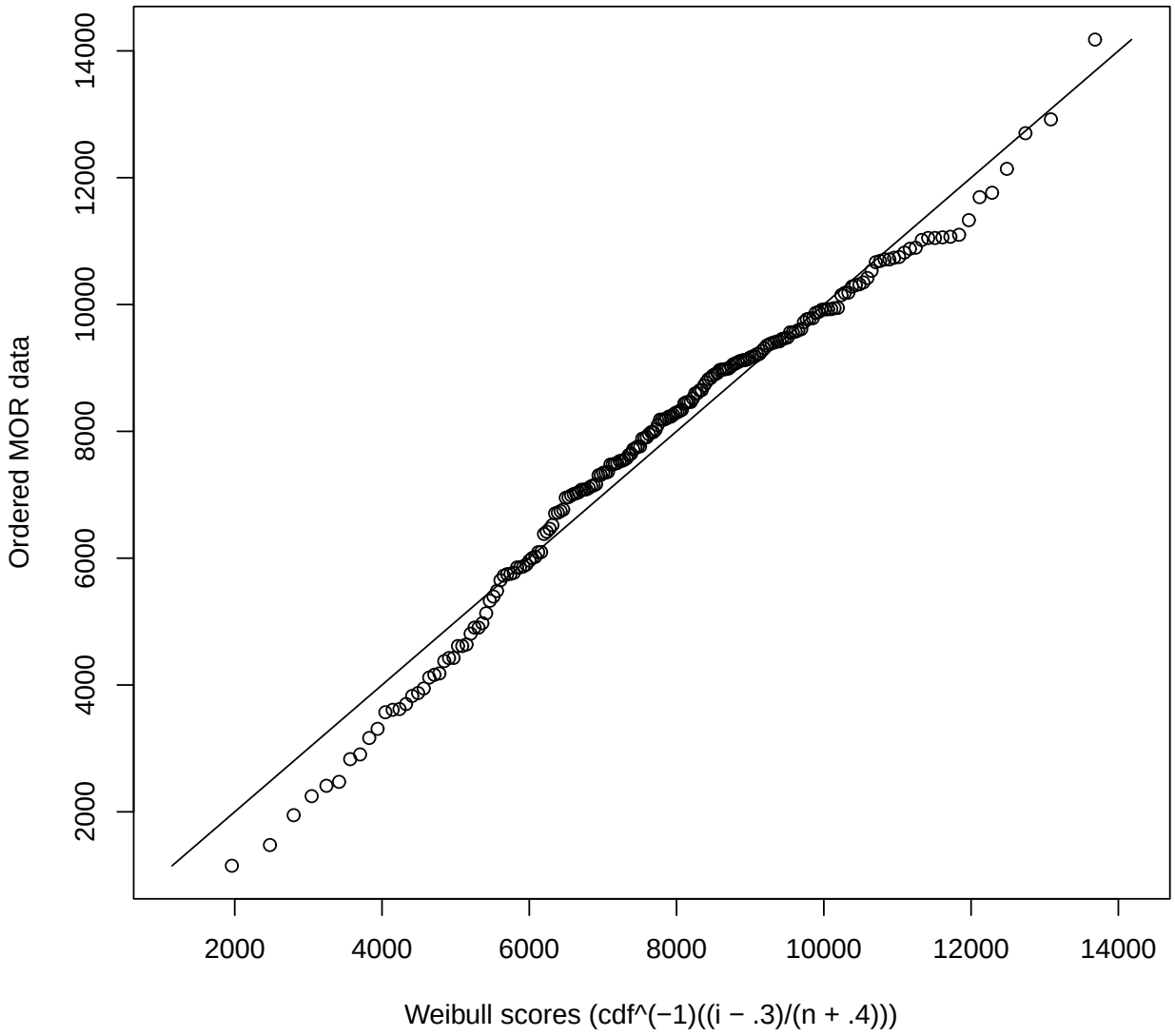

Figure 20: MOR. Ordered data versus predicted ordered data under the fitted Weibull model. The solid line is the $y = x$ line. If a Weibull model is appropriate, the plotted data points will lie approximately along the $y = x$ line.

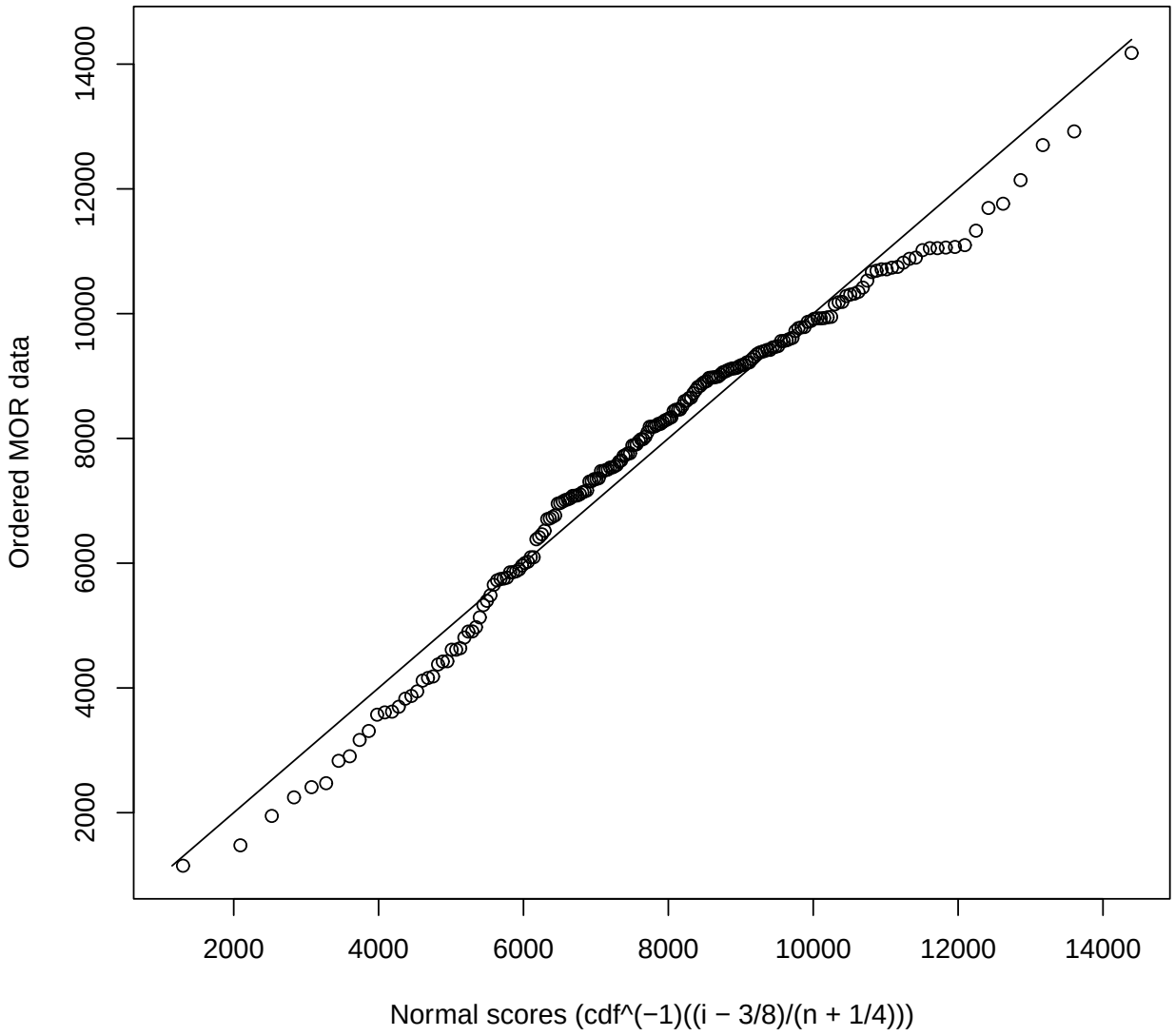

Figure 21: MOR. Ordered data versus predicted ordered data under the fitted normal model. The solid line is the $y = x$ line. If a normal model is appropriate, the plotted data points will lie approximately along the $y = x$ line.

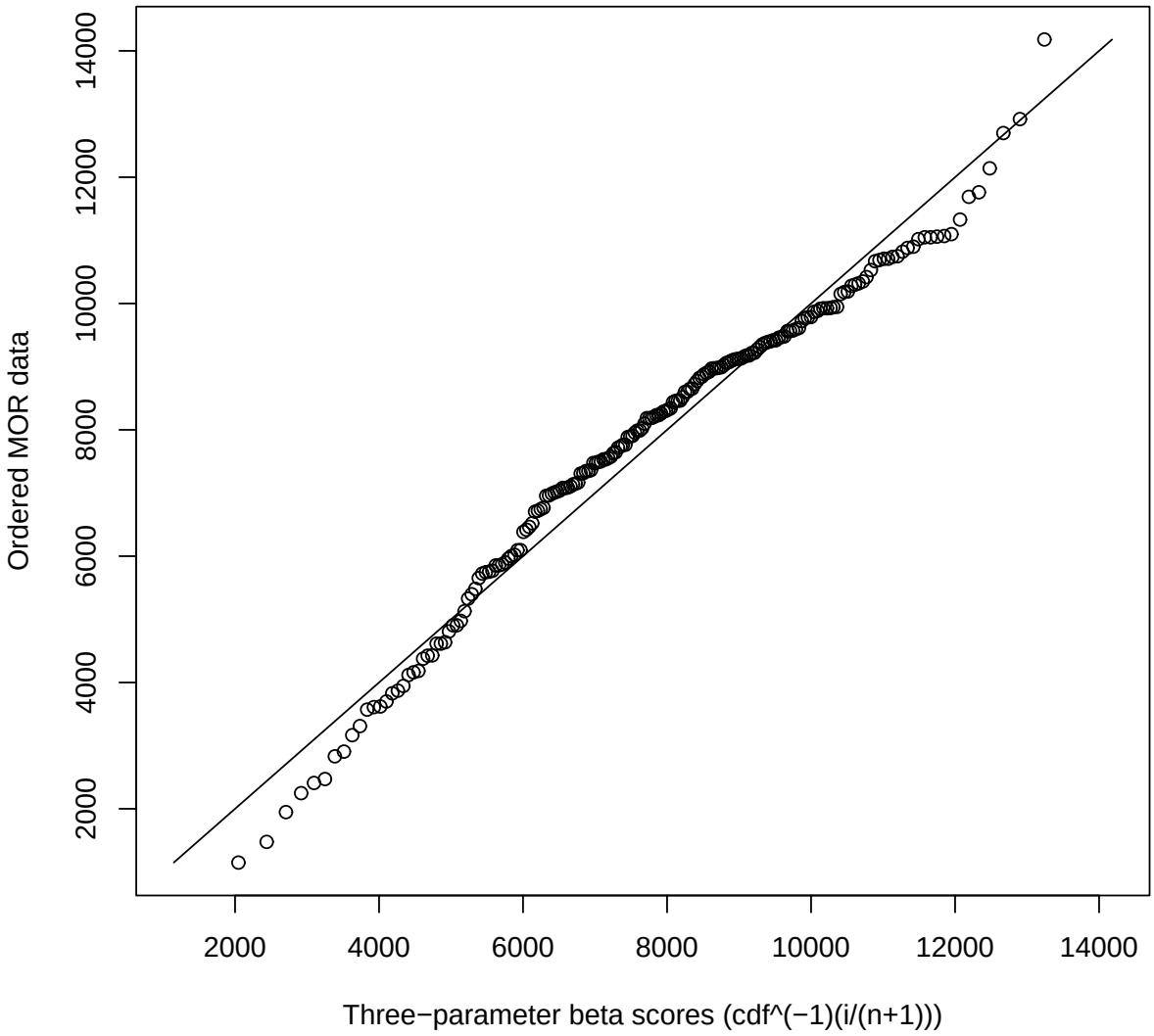

Figure 22: MOR. Ordered data versus predicted ordered data under the fitted three-parameter beta model. The solid line is the $y = x$ line. If a three-parameter beta is appropriate, the plotted data points will lie approximately along the $y = x$ line.

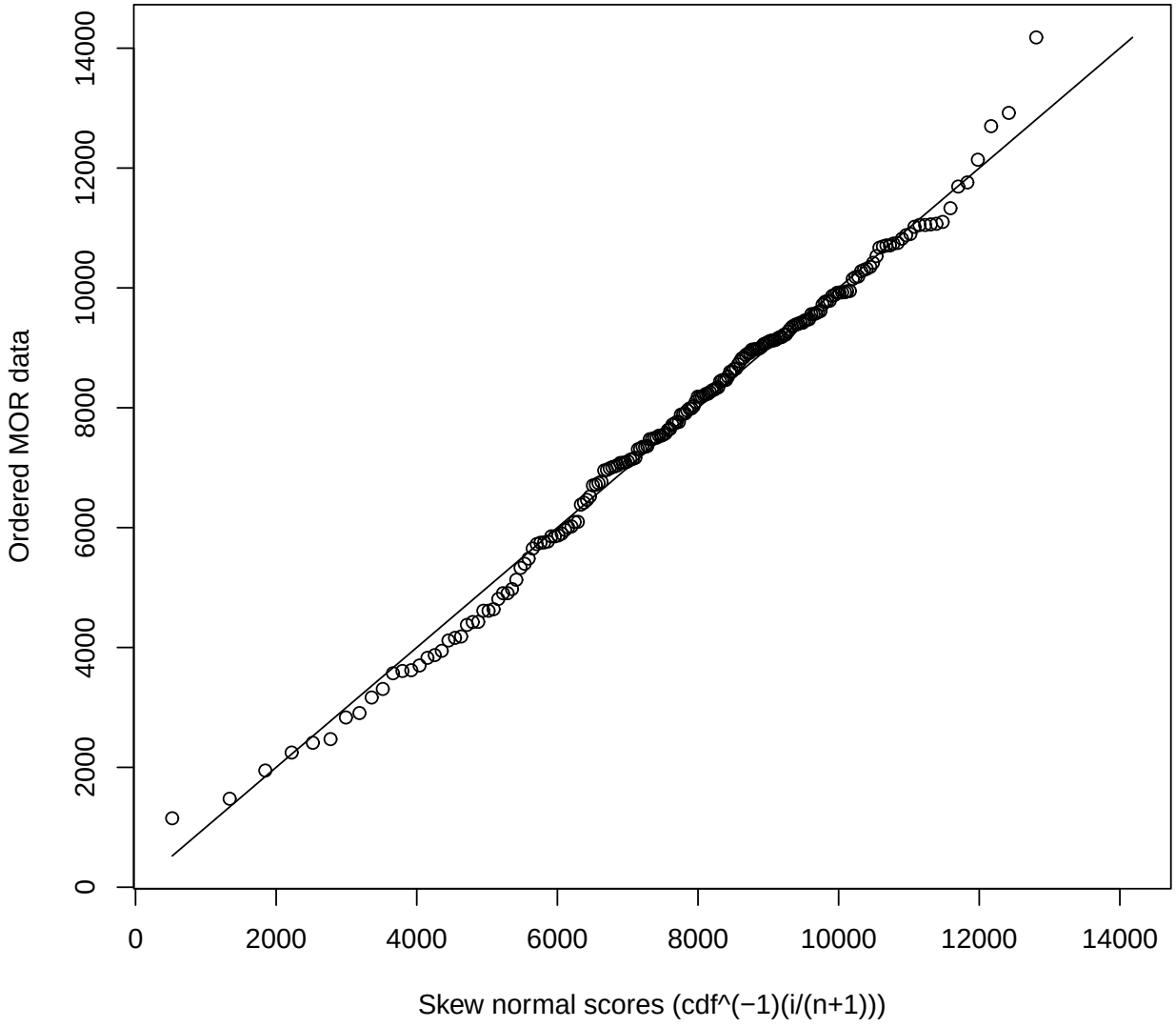

Figure 23: MOR. Ordered data versus predicted ordered data under the fitted skew normal model. The solid line is the $y = x$ line. If a skew normal model is appropriate, the plotted data points will lie approximately along the $y = x$ line.

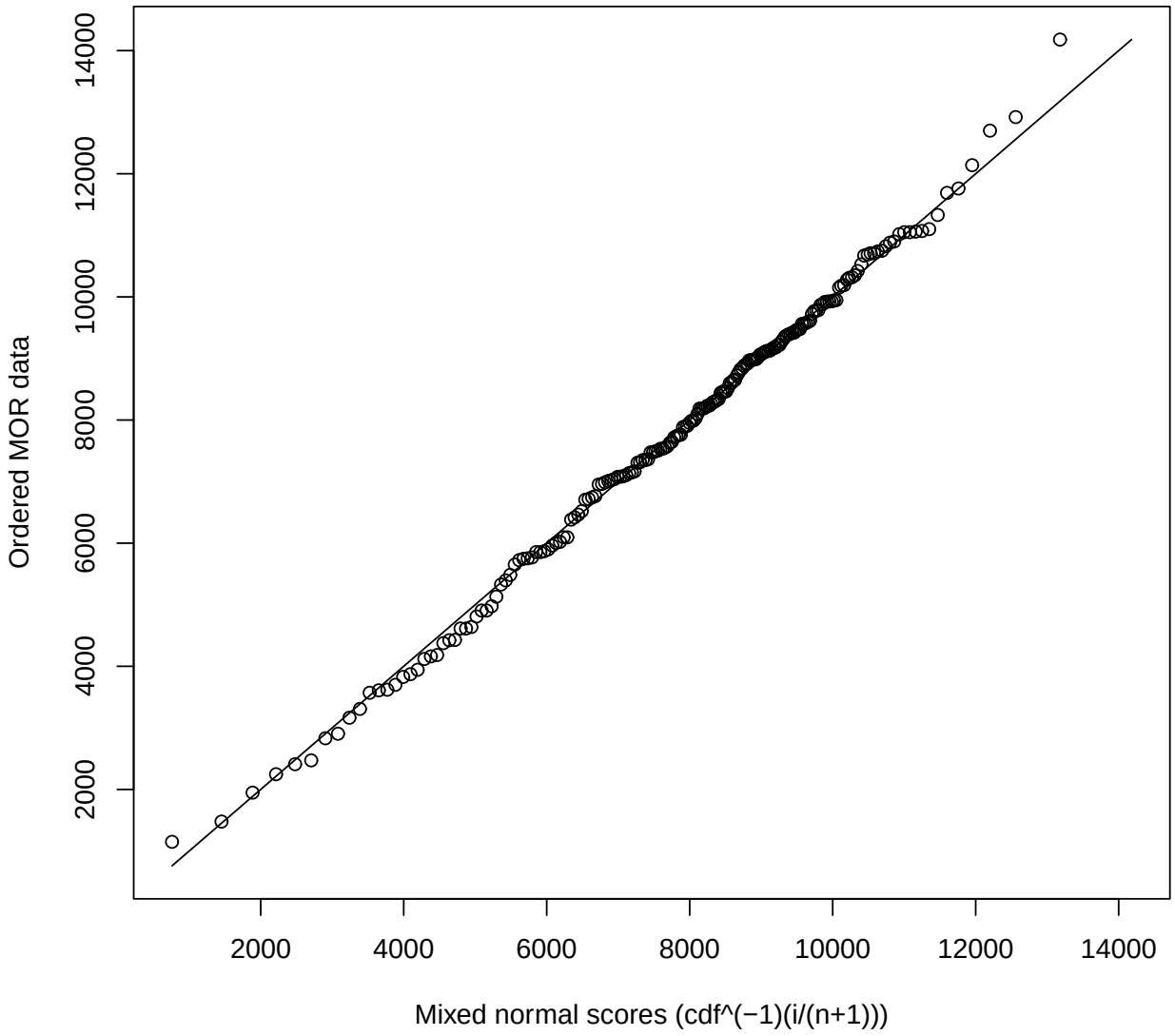

Figure 24: MOR. Ordered data versus predicted ordered data under the fitted mixed normal model. The solid line is the $y = x$ line. If a mixed normal model is appropriate, the plotted data points will lie approximately along the $y = x$ line.

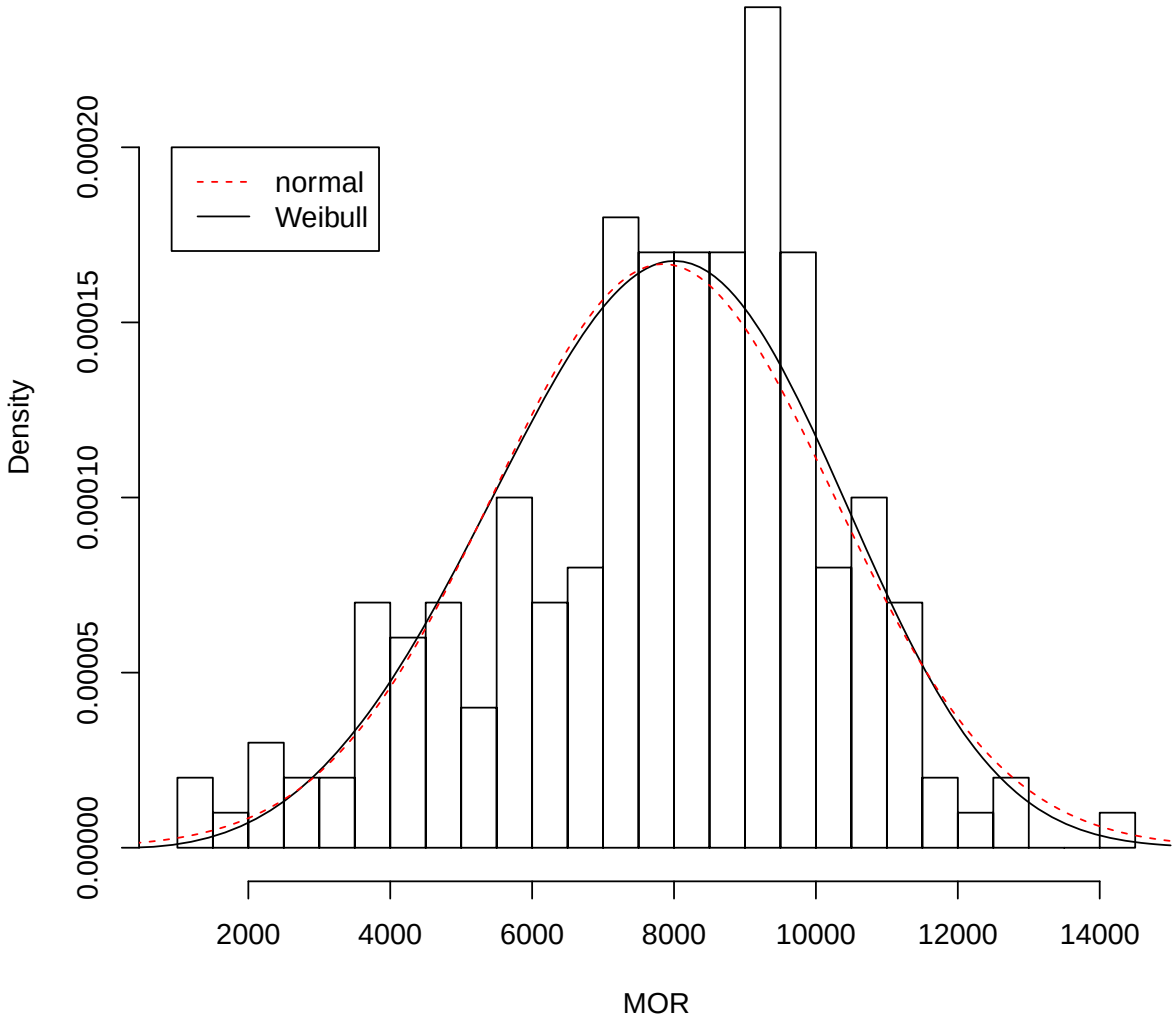

Figure 25: Histogram of the MOR data overlaid with the fitted normal and Weibull probability density functions.

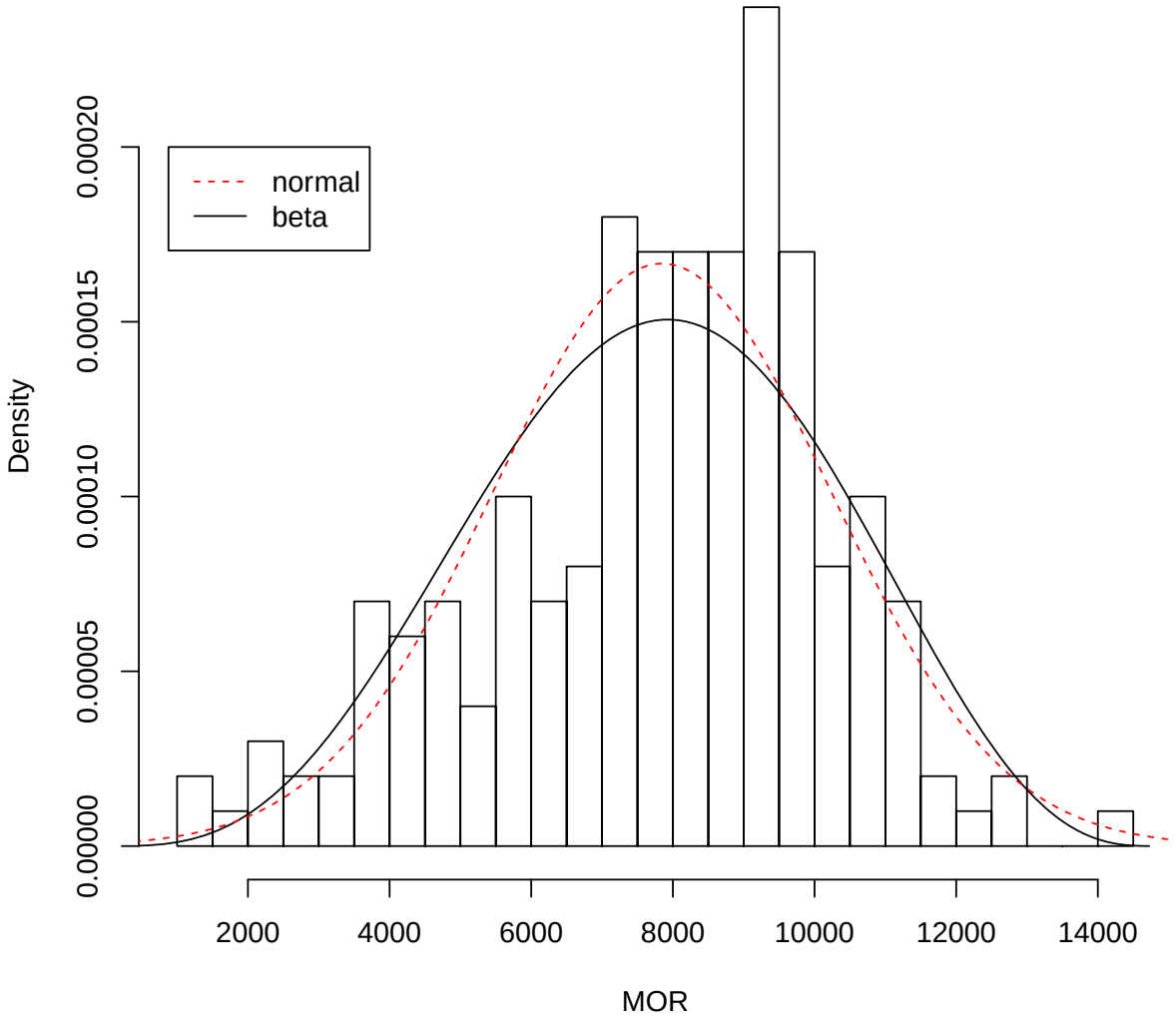

Figure 26: Histogram of the MOR data overlaid with the fitted normal and three-parameter beta probability density functions.

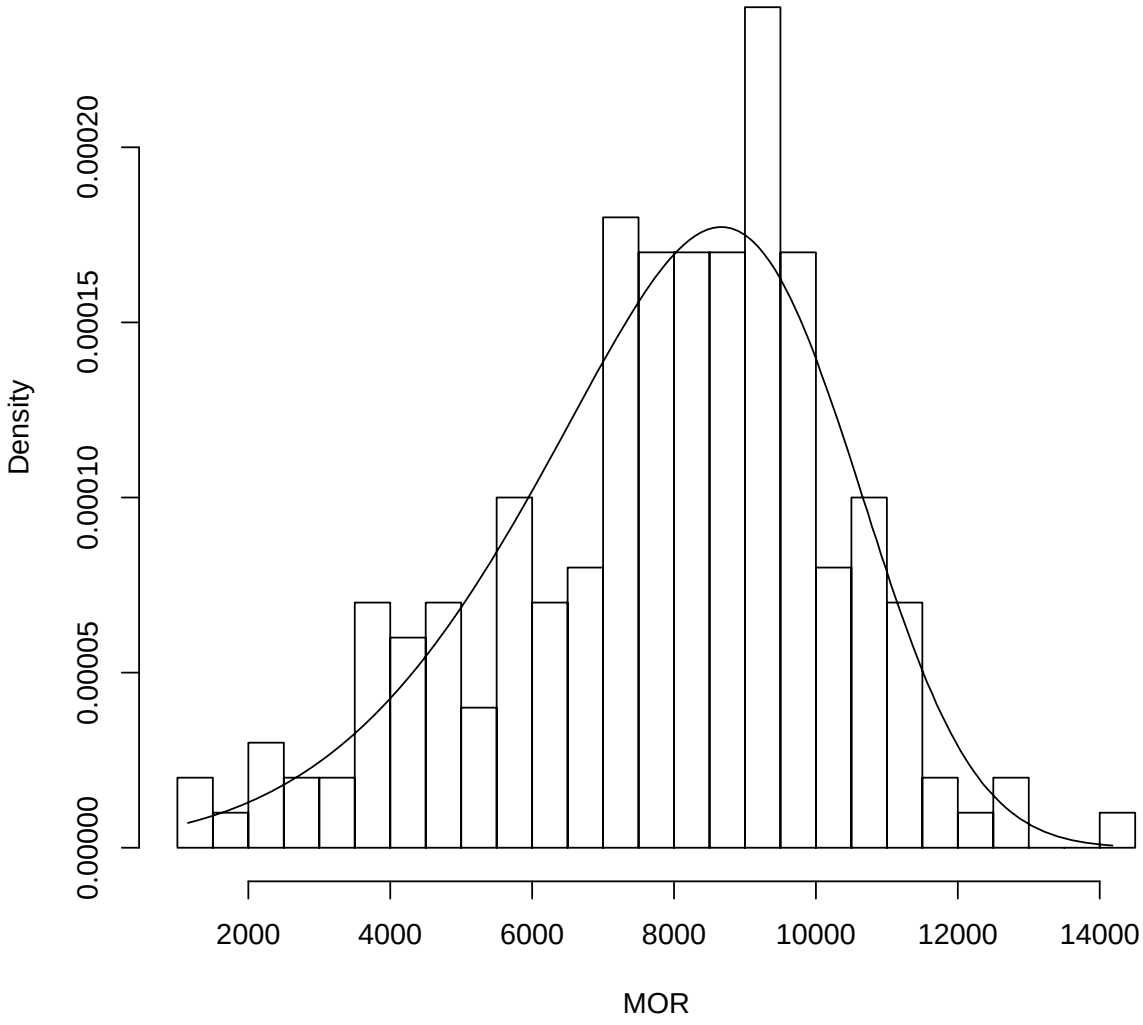

Figure 27: Histogram of the MOR data overlaid with the fitted skew normal probability density function.

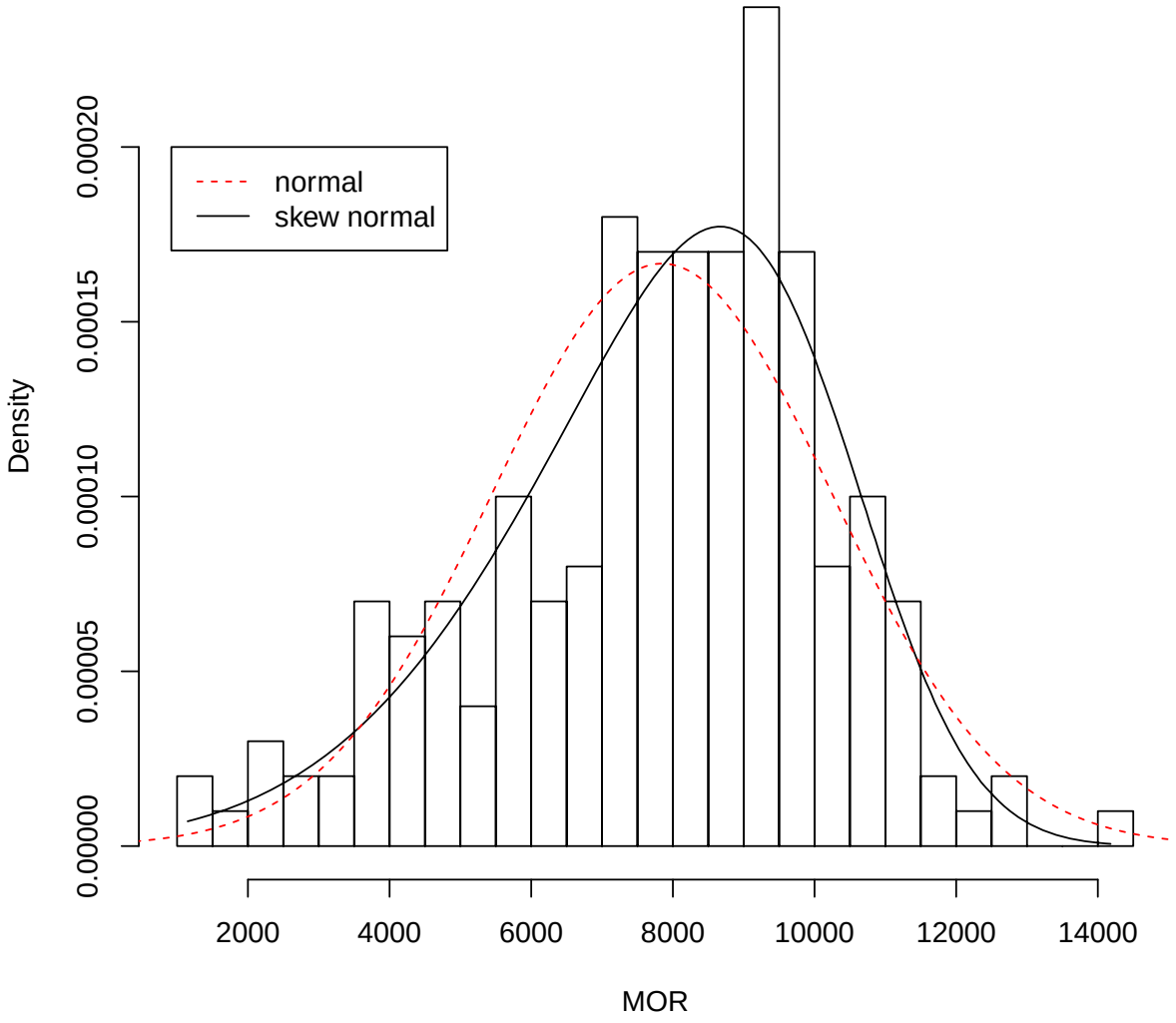

Figure 28: Histogram of the MOR data overlaid with the fitted normal and skew normal probability density functions.

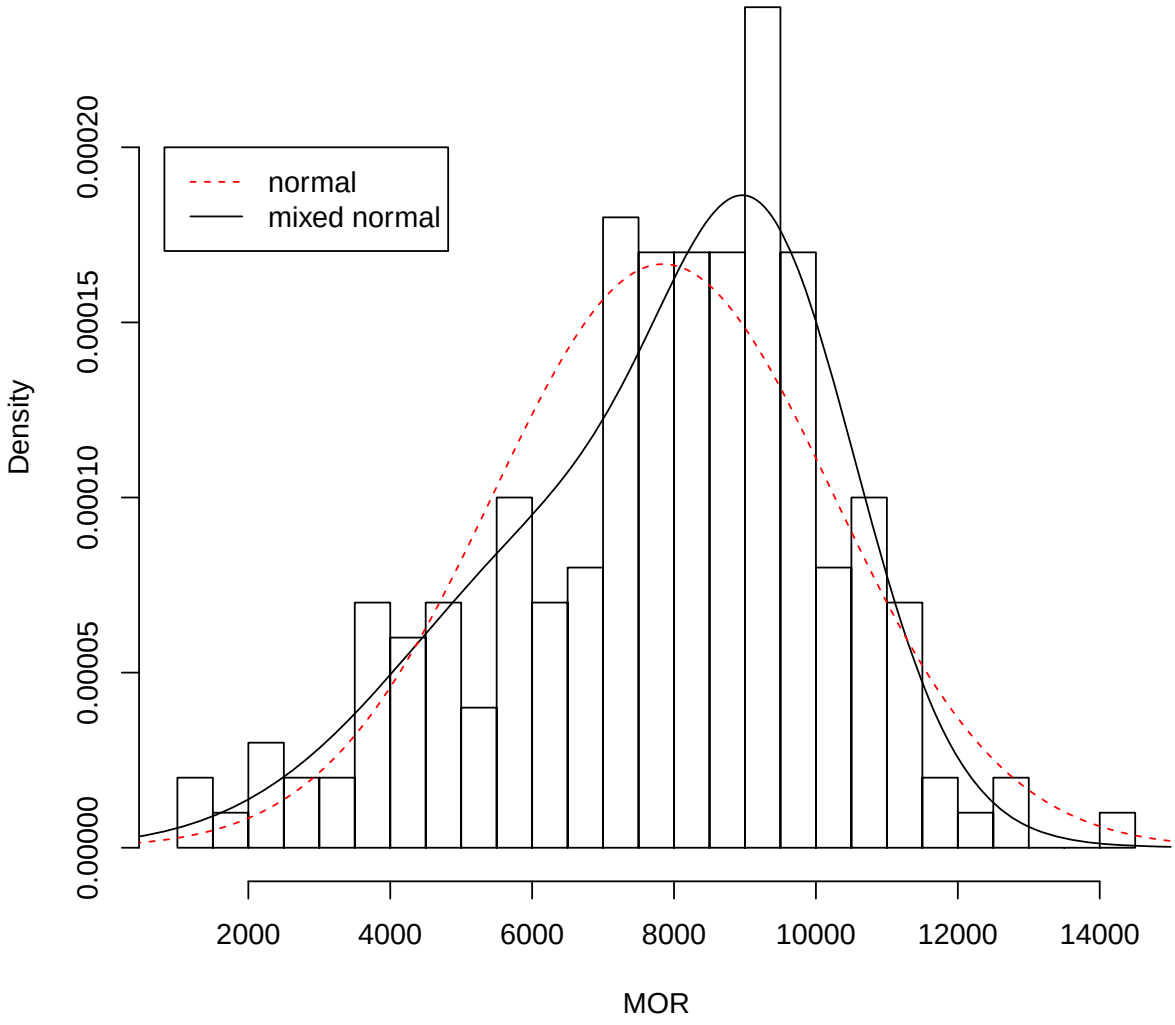

Figure 29: Histogram of the MOR data overlaid with the fitted normal and mixed normal probability density functions.

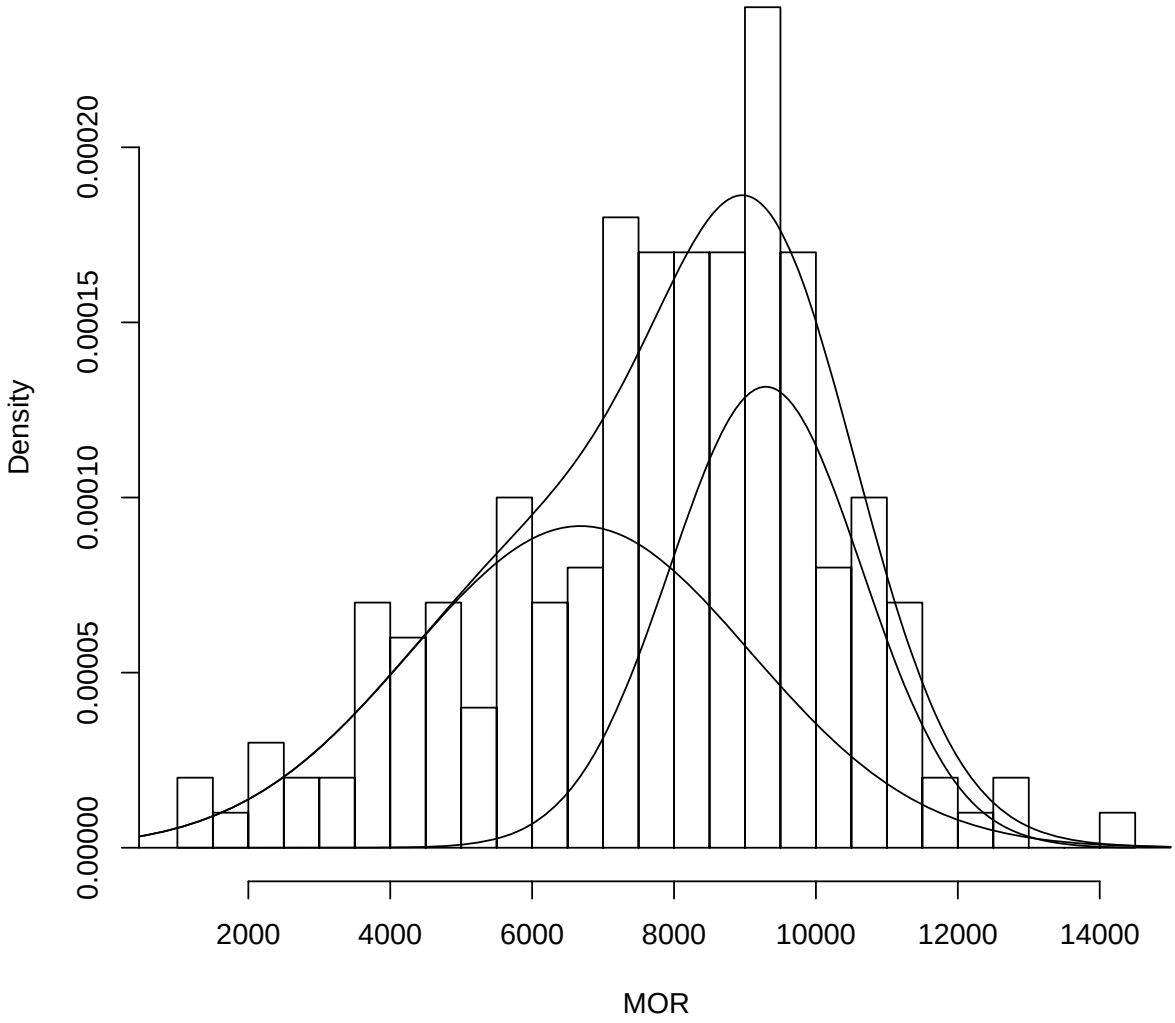

Figure 30: Histogram of the MOR data overlaid with the mixed normal probability density function and its two components.

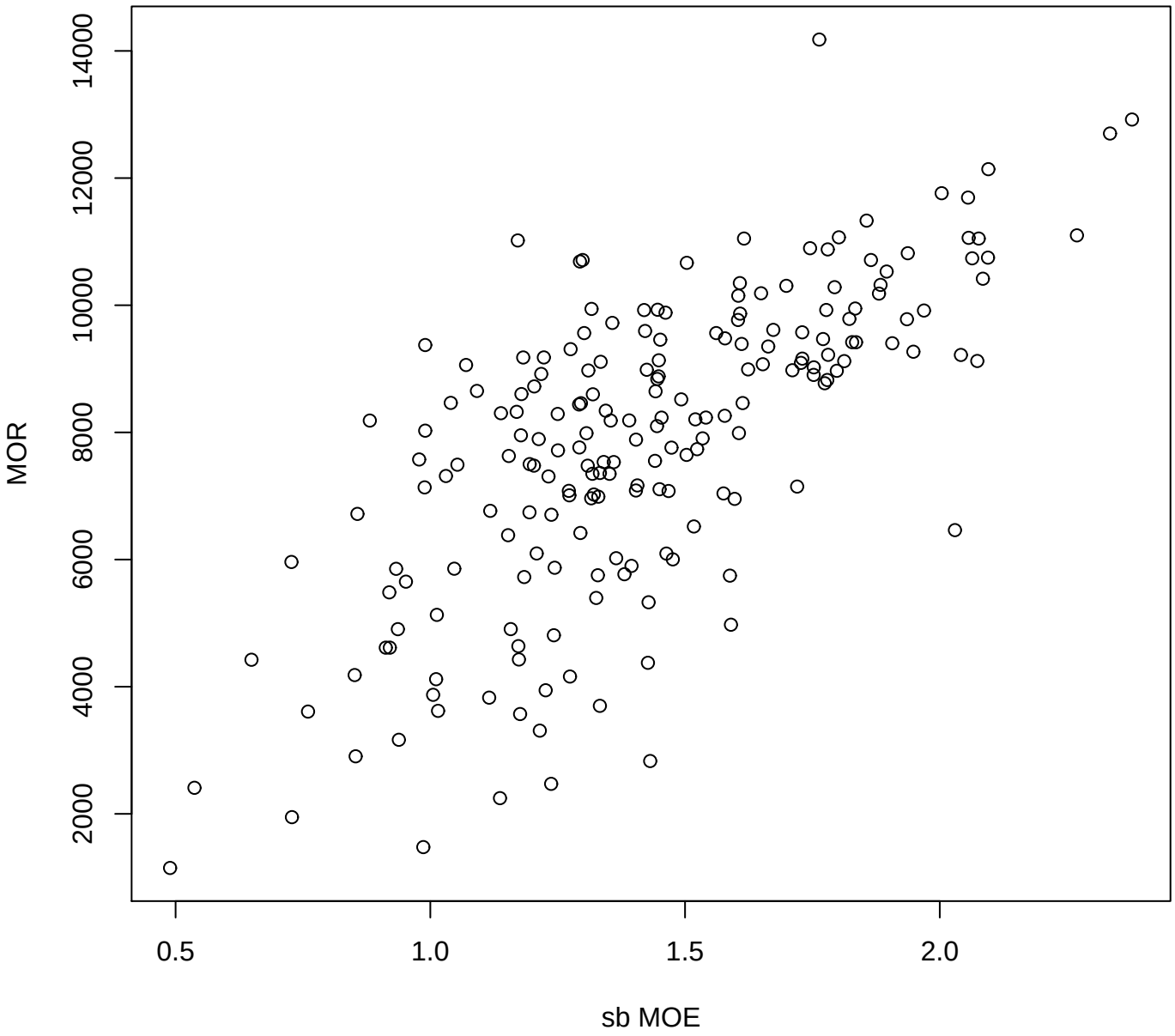

Figure 31: MOR versus sb MOE.

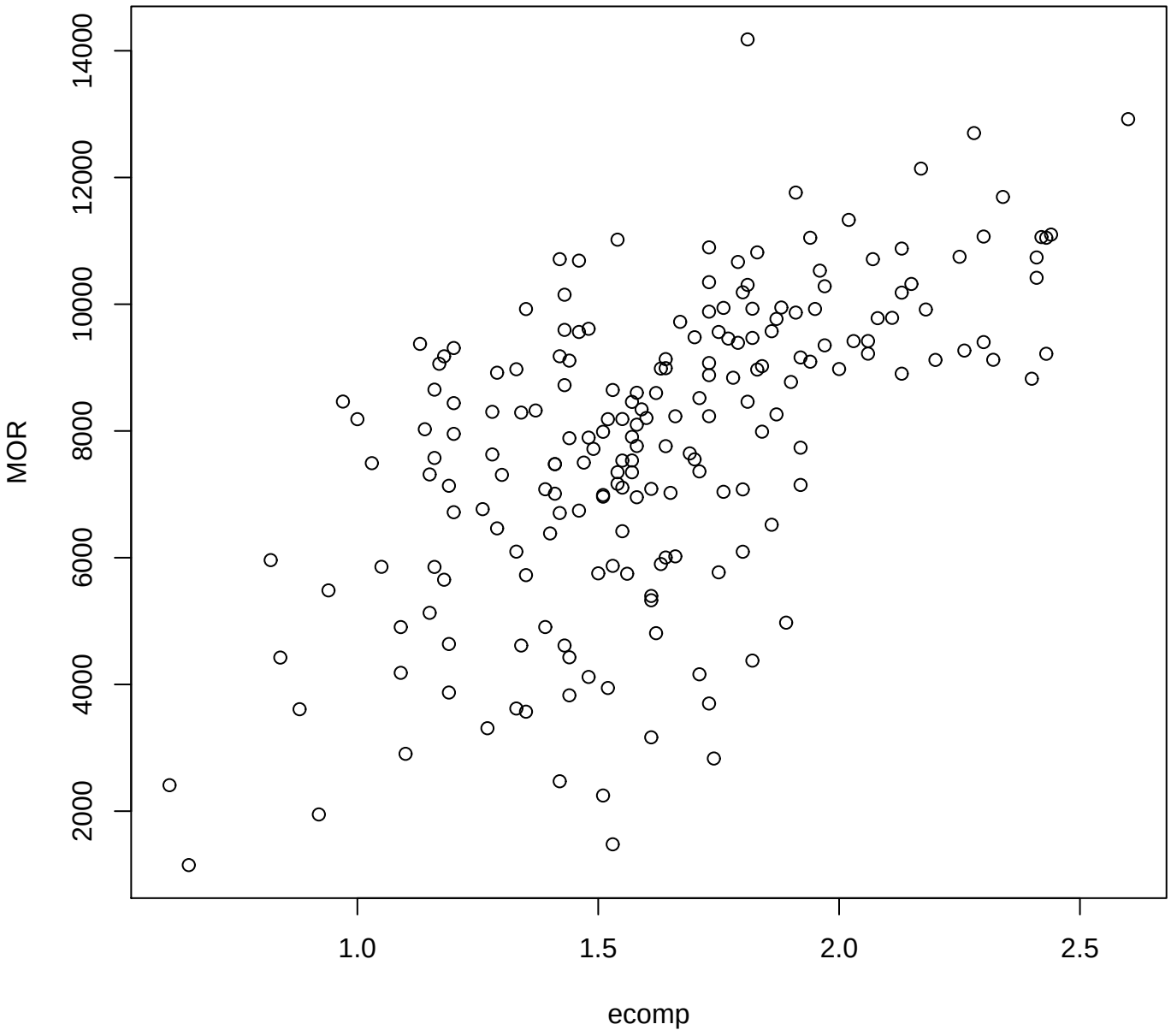

Figure 32: MOR versus ecomp.

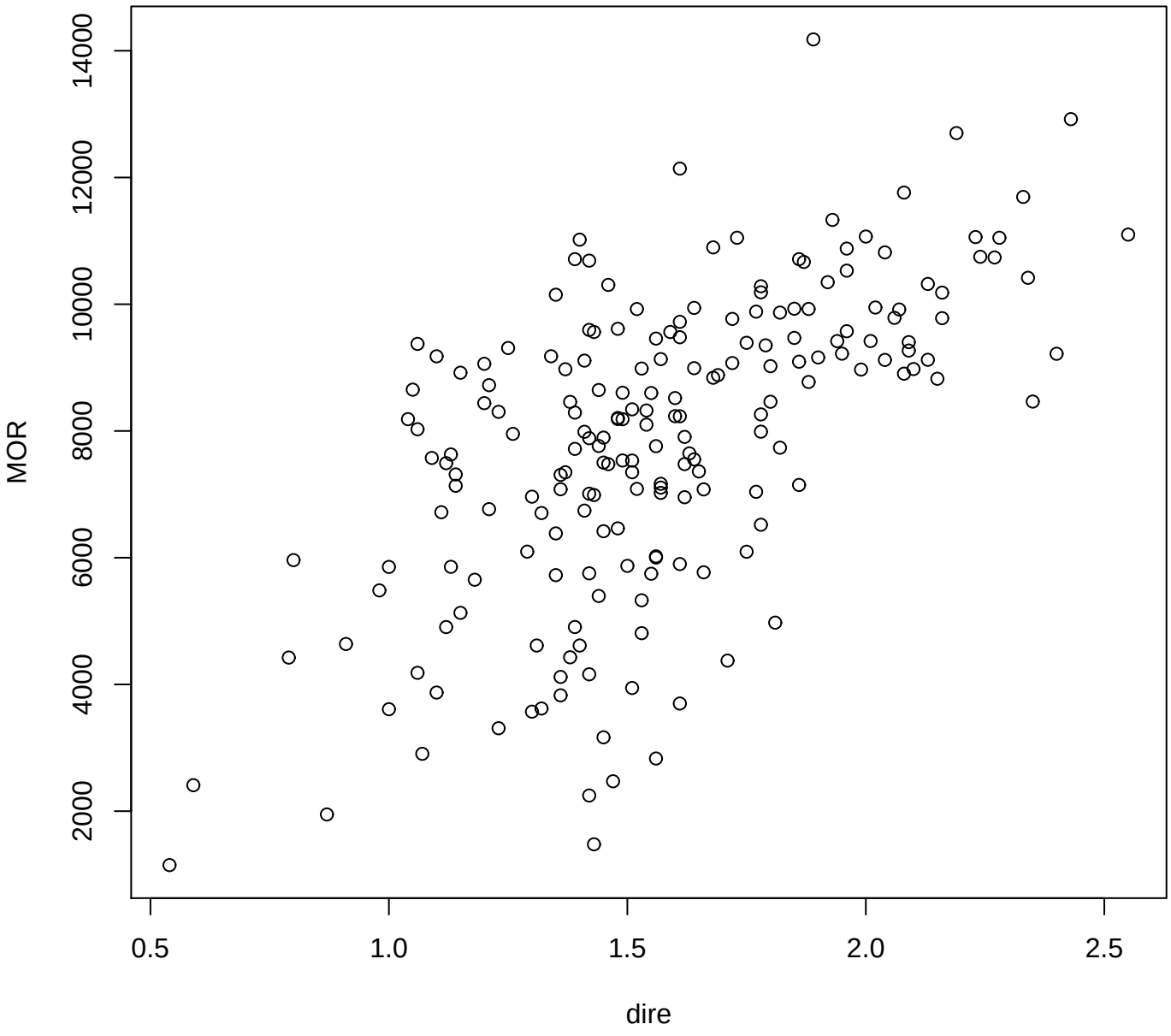

Figure 33: MOR versus dire.

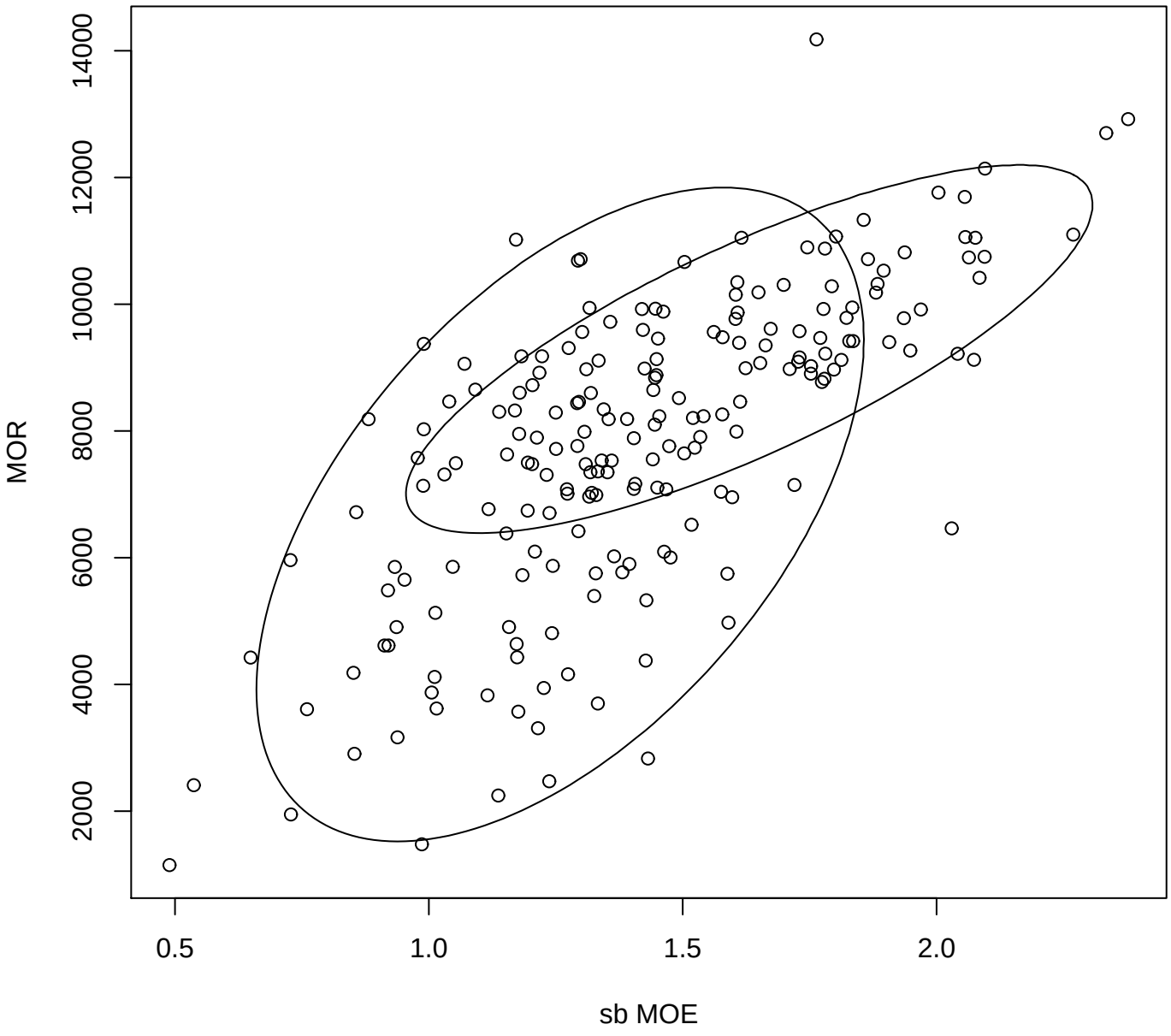

Figure 34: Scatter plot of MOR versus sb MOE, and 0.90 probability content contours for the two bivariate normal components of the fitted mixed bivariate normal model.

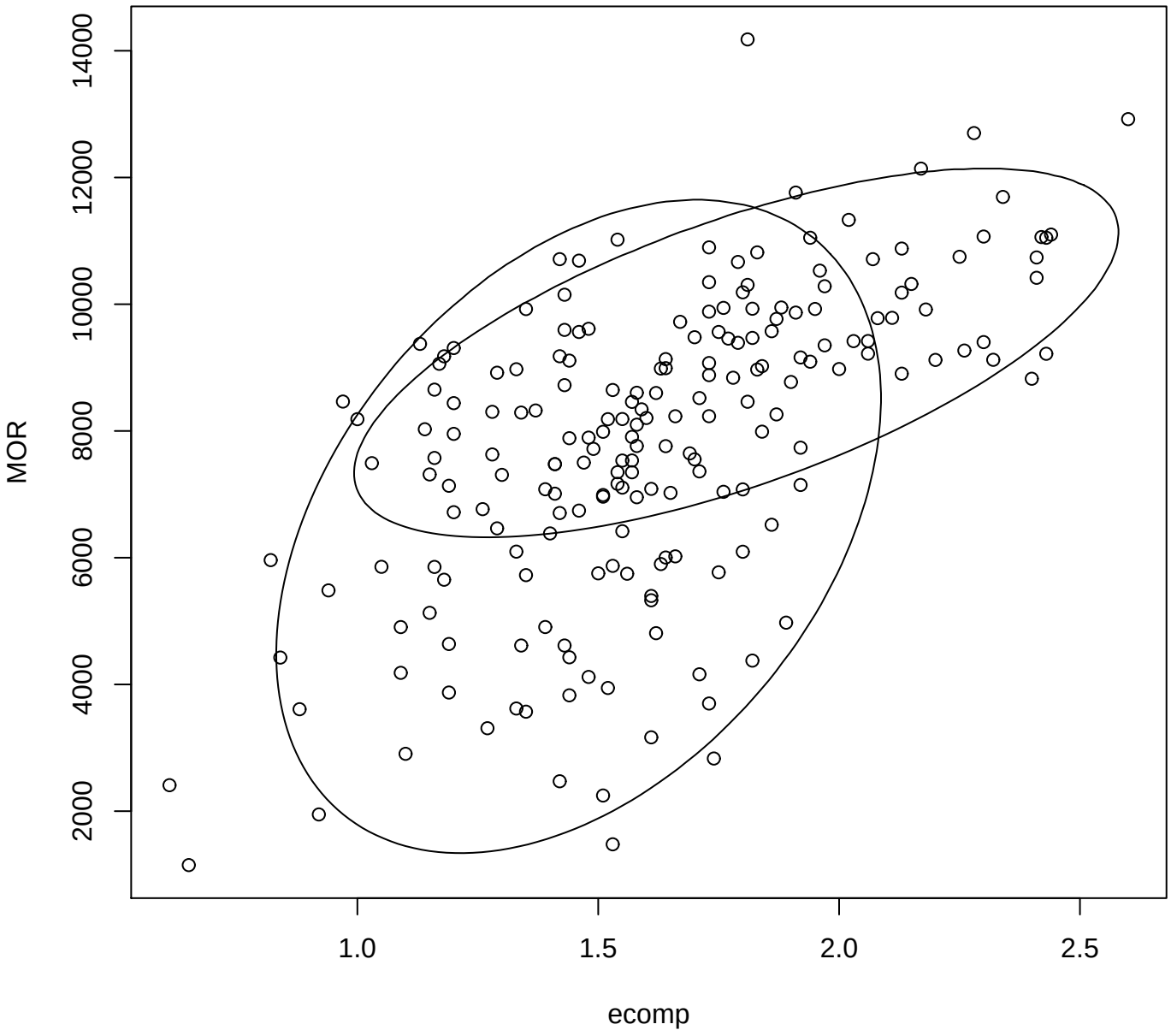

Figure 35: Scatter plot of MOR versus ecomp, and 0.90 probability content contours for the two bivariate normal components of the fitted mixed bivariate normal model.

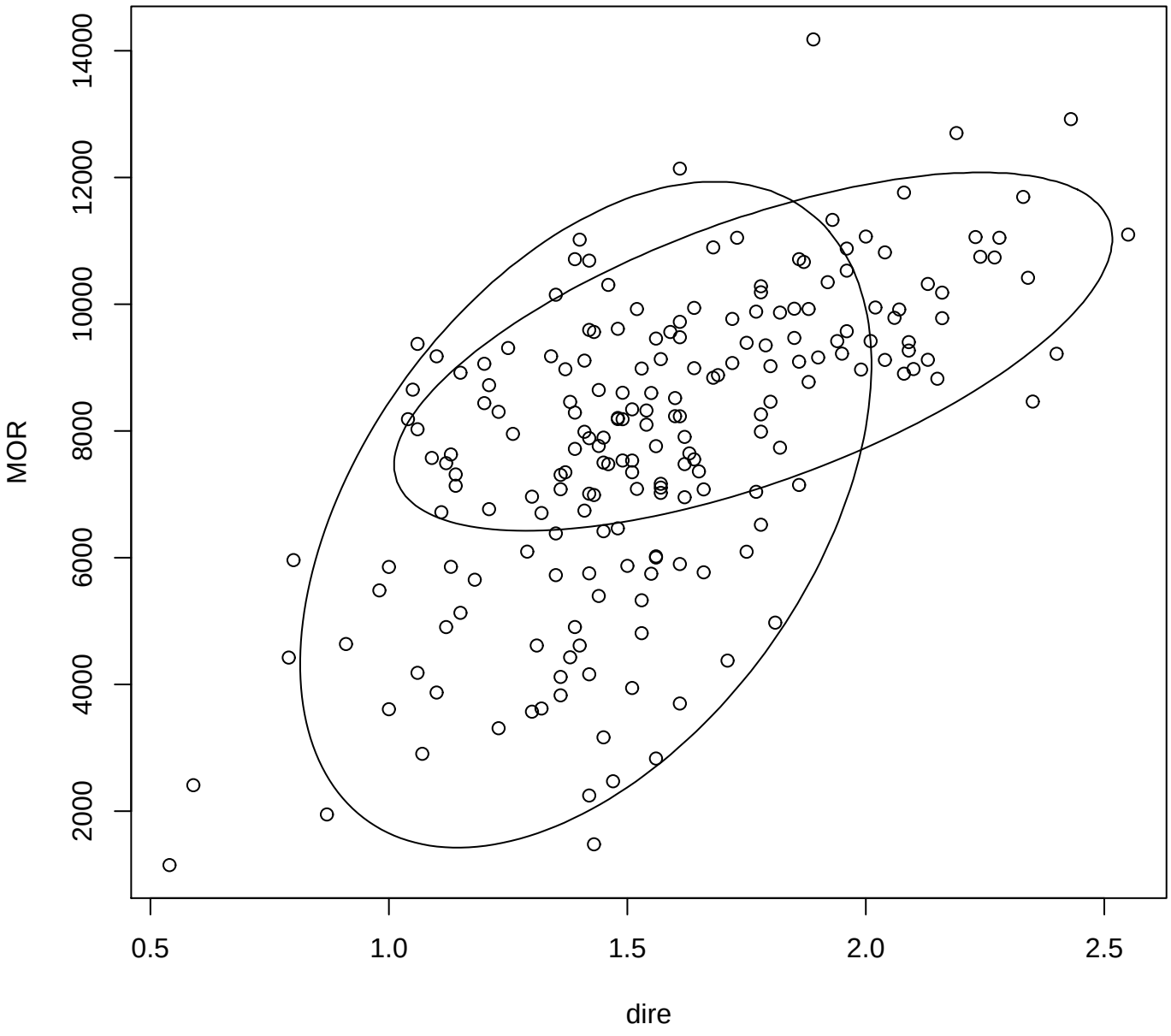

Figure 36: Scatter plot of MOR versus dire, and 0.90 probability content contours for the two bivariate normal components of the fitted mixed bivariate normal model.

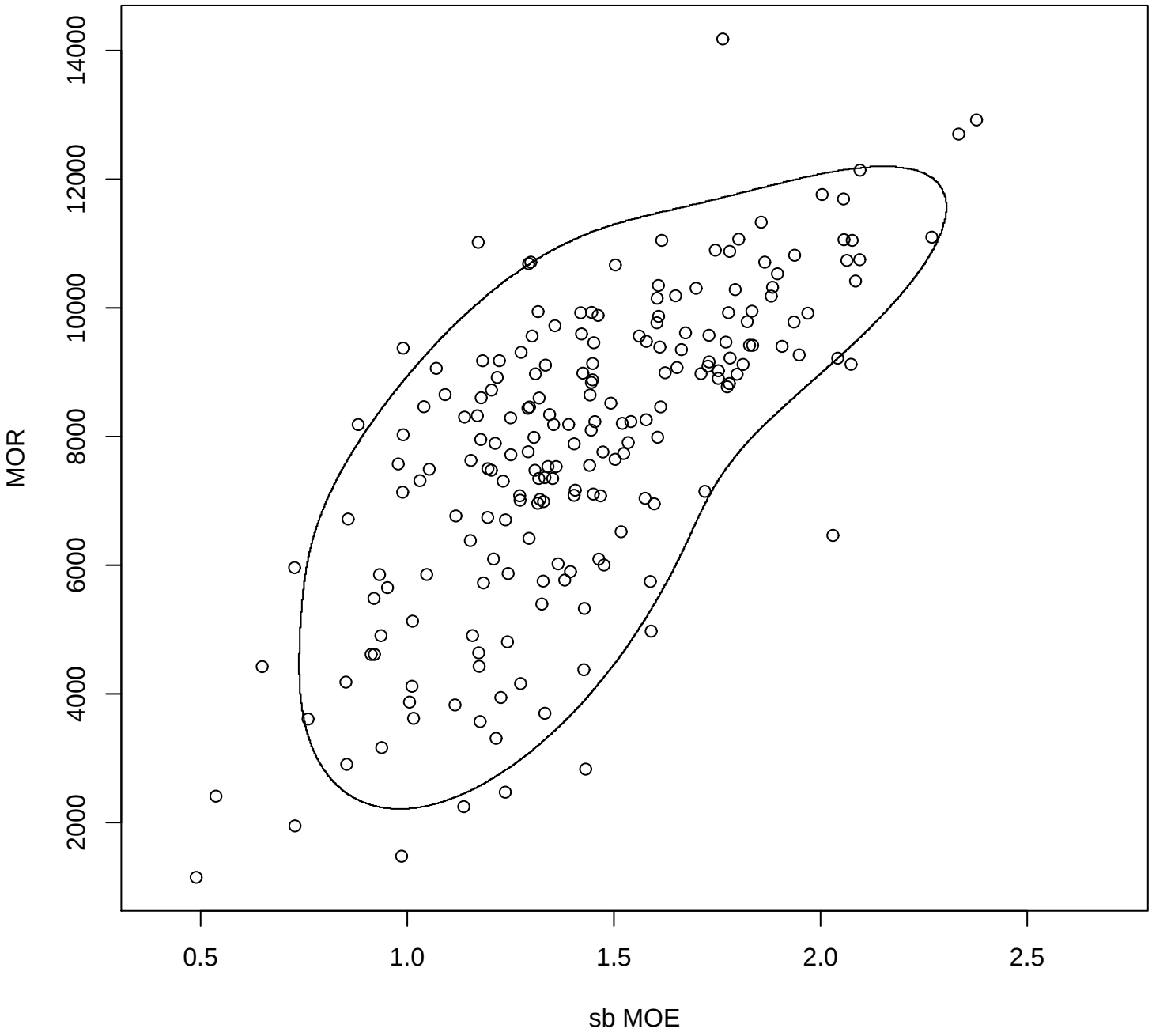

Figure 37: Scatter plot of MOR versus sb MOE, and approximate 0.90 probability content contour for the fitted full mixed bivariate normal model.

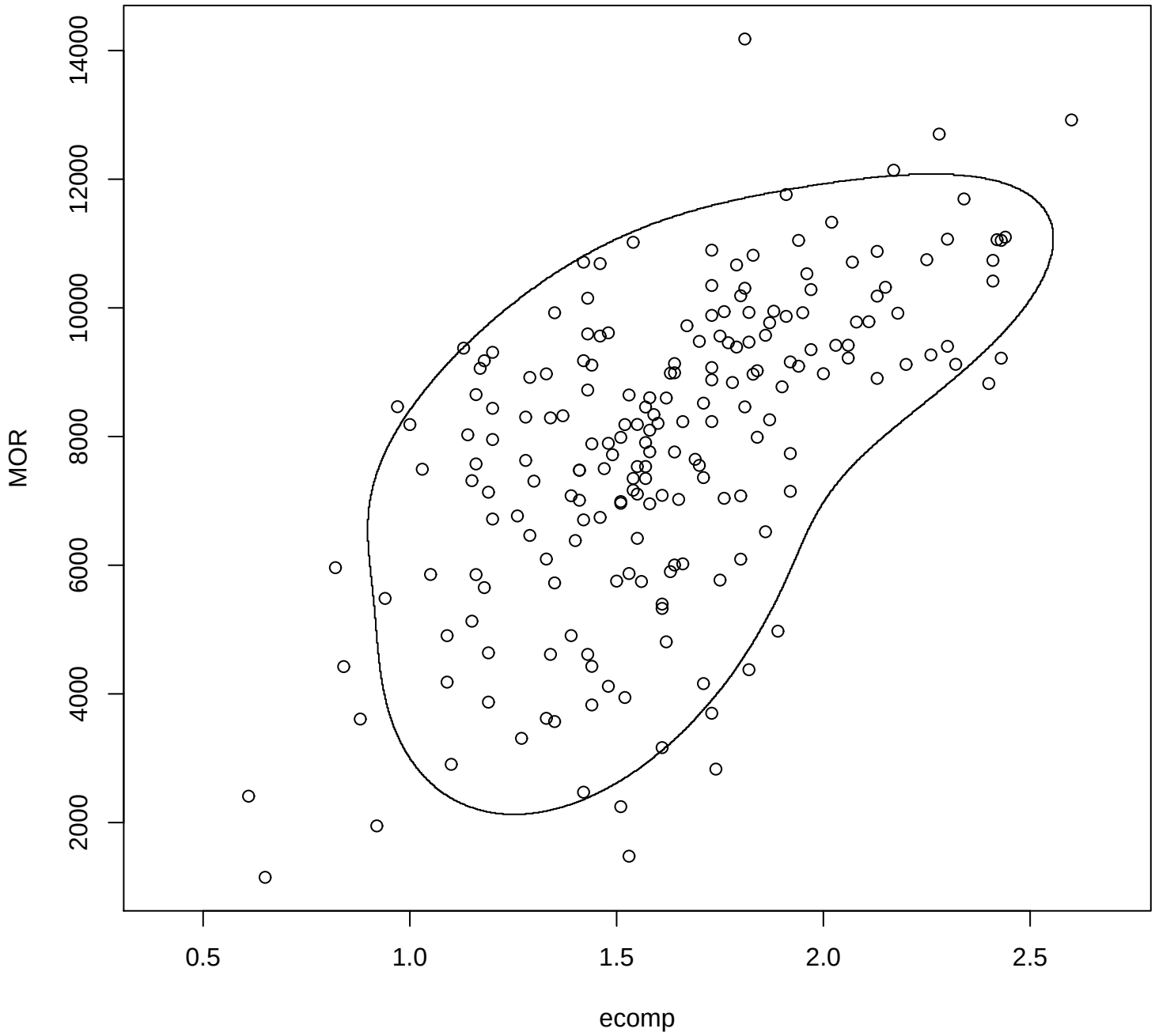

Figure 38: Scatter plot of MOR versus ecomp, and approximate 0.90 probability content contour for the fitted full mixed bivariate normal model.

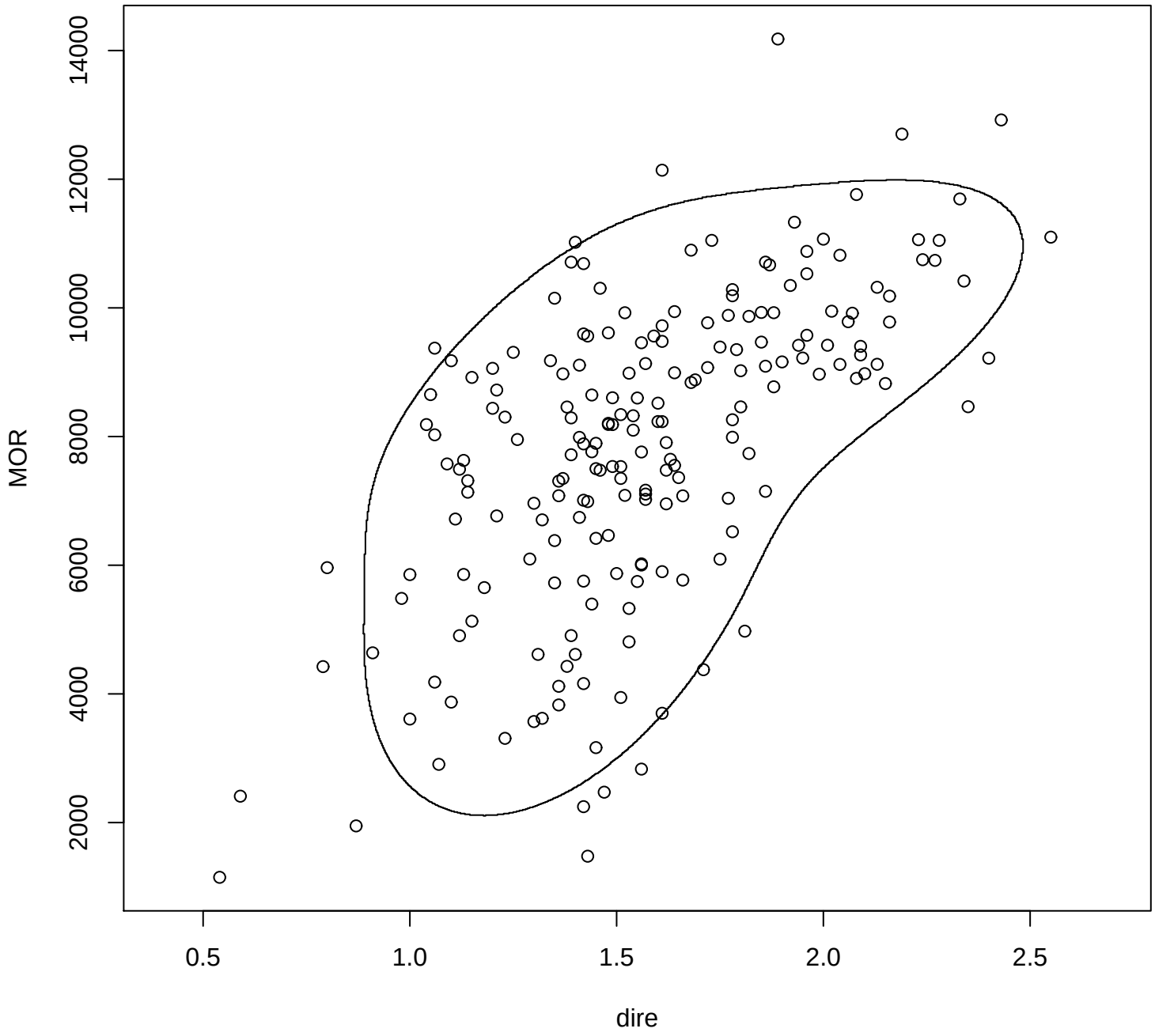

Figure 39: Scatter plot of MOR versus dire, and approximate 0.90 probability content contour for the fitted full mixed bivariate normal model.